2016-09

OPTIMIZATION OF INTER-CUBESAT COMMUNICATION LINKS

Lin, Jianwen

Monterey, California. Naval Postgraduate School

http://hdl.handle.net/10945/70982

NAVAL POSTGRADUATE SCHOOL

MONTEREY, CALIFORNIA

THESIS

OPTIMIZATION OF INTER-CUBESAT COMMUNICATION LINKS

by

Jianwen Lin

September 2016

Thesis Advisor: Weilian Su
Co-Advisor: Tri T. Ha

THIS PAGE INTENTIONALLY LEFT BLANK

REPORT DOCUMENTATION PAGE	Form Approved OMB No. 0704–0188

1. AGENCY USE ONLY *(Leave blank)*	2. REPORT DATE September 2016	3. REPORT TYPE AND DATES COVERED Master's thesis

4. TITLE AND SUBTITLE
OPTIMIZATION OF INTER-CUBESAT COMMUNICATION LINKS

5. FUNDING NUMBERS

6. AUTHOR(S) Jianwen Lin

7. PERFORMING ORGANIZATION NAME(S) AND ADDRESS(ES)
Naval Postgraduate School
Monterey, CA 93943-5000

8. PERFORMING ORGANIZATION REPORT NUMBER

9. SPONSORING /MONITORING AGENCY NAME(S) AND ADDRESS(ES)
N/A

10. SPONSORING / MONITORING AGENCY REPORT NUMBER

11. SUPPLEMENTARY NOTES The views expressed in this thesis are those of the author and do not reflect the official policy or position of the Department of Defense or the U.S. Government. IRB number ____N/A____.

12a. DISTRIBUTION / AVAILABILITY STATEMENT
Approved for public release. Distribution is unlimited.

12b. DISTRIBUTION CODE

13. ABSTRACT (maximum 200 words)

Cubesat constellations may become the next generation of communication backbone architecture to provide future worldwide communication services. In this thesis, we investigate the feasibility of deploying Cubesat constellations with inter-satellite links (ISL) for the delivery of continuous global communication. Cubesat constellation designs for various mission scenarios are proposed and verified using a simulation toolkit commonly used by space engineers. Link optimization to improve the overall theoretical data rate is also discussed. The results obtained affirm that a Cubesat constellation at an orbital height of 450 km can achieve a data rate of 11.46 kbps and requires the least number of satellites in the constellation. We ascertained that using ISL as the communication backbone in a network architecture, complete with space and globally distributed ground nodes, is achievable. In the near future, there is a high potential for the implementation of ISL with optical communication links, whereby there is assurance of a significantly higher data rate and lower power requirements.

14. SUBJECT TERMS
Cubesat, Constellations, inter-satellite link

15. NUMBER OF PAGES
111

16. PRICE CODE

17. SECURITY CLASSIFICATION OF REPORT	18. SECURITY CLASSIFICATION OF THIS PAGE	19. SECURITY CLASSIFICATION OF ABSTRACT	20. LIMITATION OF ABSTRACT
Unclassified	Unclassified	Unclassified	UU

NSN 7540–01-280-5500

Standard Form 298 (Rev. 2–89)
Prescribed by ANSI Std. 239–18

THIS PAGE INTENTIONALLY LEFT BLANK

Approved for public release. Distribution is unlimited.

OPTIMIZATION OF INTER-CUBESAT COMMUNICATION LINKS

Jianwen Lin
Civilian, Singapore Technologies Electronics
B.S.E.E., Nanyang Technological University, 2007

Submitted in partial fulfillment of the
requirements for the degree of

MASTER OF SCIENCE IN ELECTRICAL ENGINEERING

from the

NAVAL POSTGRADUATE SCHOOL
September 2016

Approved by: Weilian Su
Thesis Advisor

Tri T. Ha
Co-Advisor

R. Clark Robertson
Chair, Department of Electrical and Computer Engineering

THIS PAGE INTENTIONALLY LEFT BLANK

ABSTRACT

Cubesat constellations may become the next generation of communication backbone architecture to provide future worldwide communication services. In this thesis, we investigate the feasibility of deploying Cubesat constellations with inter-satellite links (ISL) for the delivery of continuous global communication. Cubesat constellation designs for various mission scenarios are proposed and verified using a simulation toolkit commonly used by space engineers. Link optimization to improve the overall theoretical data rate is also discussed. The results obtained affirm that a Cubesat constellation at an orbital height of 450 km can achieve a data rate of 11.46 kbps and requires the least number of satellites in the constellation. We ascertained that using ISL as the communication backbone in a network architecture, complete with space and globally distributed ground nodes, is achievable. In the near future, there is a high potential for the implementation of ISL with optical communication links, whereby there is assurance of a significantly higher data rate and lower power requirements.

THIS PAGE INTENTIONALLY LEFT BLANK

TABLE OF CONTENTS

LIST OF FIGURES

LIST OF TABLES

THIS PAGE INTENTIONALLY LEFT BLANK

LIST OF ACRONYMS AND ABBREVIATIONS

ATP	acquisition, tracking, and pointing
BFSK	binary frequency-shift keying
BLOS	beyond line-of-sight
BPSK	binary phase-shift keying
COTS	commercial off-the-shelf
CSK	code-shift keying
EIRP	effective isotropic radiated power
FSK	frequency-shift keying
GEO	geostationary-earth orbit
GPS	global positioning systems
ISL	inter-satellite links
LEO	low-earth orbit
LOS	line-of-sight
MCSK	M-ary code-shift keying
MEO	medium-earth orbit
MFSK	M-ary frequency-shift keying
MPSK	M-ary phase-shift keying
NASA	National Aeronautics and Space Administration
OPALS	Optical Payload for Lasercomm Science
PSK	phase-shift keying
QPSK	quadrature phase-shift keying
RF	radio frequency
SOC	street-of-coverage
STK	Systems Tool Kit
UAV	unmanned aerial vehicle
UHF	ultra high frequency

THIS PAGE INTENTIONALLY LEFT BLANK

ACKNOWLEDGMENTS

I would like to express my gratitude to both my thesis advisor, Professor Weilian Su, and co-advisor, Professor Tri T. Ha, for their invaluable guidance toward the development of this thesis. Their continuous support throughout my research, constant assurance of my progress, and help in keeping me on track have been essential in the success of my thesis.

Next, to my beautiful and understanding wife, Yanmin, who has constantly been supporting and encouraging me. My success in the Naval Postgraduate School would not be possible without her managing the family well so that I can focus on my studies.

I am also thankful to have my daughter, Jerrine, who has brought so much love, laughter, and joy to my life.

Last, I wish to thank my organization, Singapore Technologies Electronics, for offering me this once-in-a-lifetime opportunity to further my studies in the United States.

THIS PAGE INTENTIONALLY LEFT BLANK

I. INTRODUCTION

Cubesats, being a cheaper alternative to traditional satellites, are gaining popularity as the next generation of satellite system by virtue of the hardware miniaturization effect made possible by technological advancements. Cubesats have changed the communication outlook from long-range, point-to-point propagation to a multi-hop network of small orbiting nodes. Numerous Cubesats, when grouped together as a constellation, can form a wireless sensor network, and the inter-satellite links (ISL) between the Cubesats in the constellation are a potential area for research.

A. BACKGROUND

In the network architecture, a robust communication channel is a cardinal requirement for reliable data transfer between nodes. For ground nodes that operate within the area-of-interest where there is a clear line-of-sight (LOS), radio communication techniques can be employed; however, when the area-of-interest is large and ground nodes are located beyond line-of-sight (BLOS), there is a need to rely on other communication techniques such as satellite communications. For this case, a satellite functions as a repeater in space to transfer data from one geographic location to another, as shown in Figure 1.

In this thesis, a Cubesat is employed as the BLOS repeater solution for communication between the space and ground segments. Since a Cubesat has a small payload and operates in low-earth orbit (LEO), the footprint coverage is limited for a single Cubesat. Moreover, based on the orbital movement for satellites deployed in LEO, the satellite coverage constantly moves, and its dwell time over a designated area is limited [1]. As a result, Cubesats must be deployed in constellations to enable continuous coverage over the designated area. Furthermore, if continuous global coverage is required, we must rely on ISL between Cubesats to provide a seamless communication channel in the space segment. The mission scenario for this analysis is shown in Figure 2.

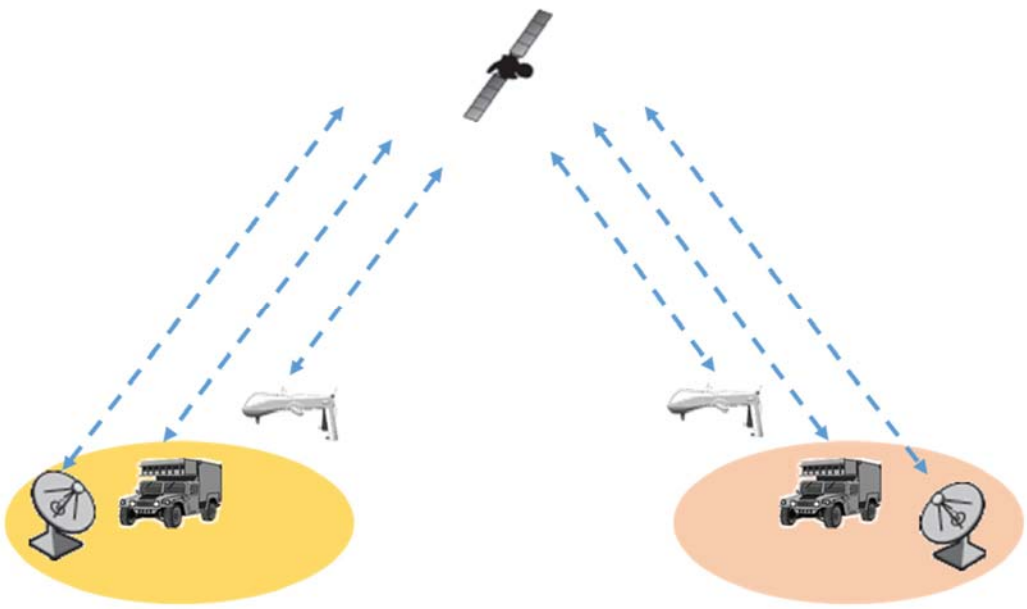

Figure 1. System Overview Using Conventional Satellite as a Repeater

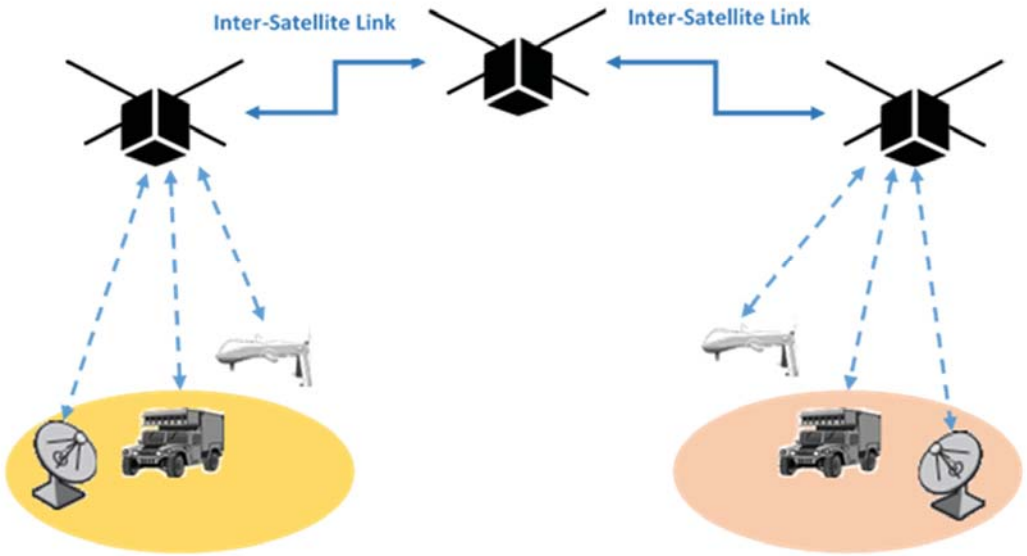

Figure 2. System Overview Using Cubesat with ISL

B. OBJECTIVES

The objectives of this thesis are to design Cubesat constellations with ISL to act as the backbone communication architecture for continuous global coverage, to propose

suitable Cubesat constellation architectures for different mission profiles, and to ensure that the Cubesat constellation design is optimized to deliver the highest data rate available to the nodes without compromising the mission requirement.

In the mission scenario investigated, Cubesats function as space repeaters, and the information collected is relayed to terrestrial nodes, which consist of Unmanned Aerial Vehicles (UAV), mobile vehicles, and ground stations. Noting the high number of Cubesats deployed to achieve continuous global coverage, we must ensure that there is a minimum separation distance between the Cubesats to avoid collision. Collisions in space are catastrophic situations, highlighting the importance of collision avoidance as a constellation design consideration.

C. LITERATURE REVIEW

To have a clearer understanding of satellite communications, research on past work in the areas related to the basic fundamentals of orbital elements and their impacts on satellite constellation design, common constellation design methods, and communications principles were performed. In addition, numerous publications on Cubesat constellations that use ISL were studied.

In [2], [3], researchers investigated the possibility of using Cubesat to relay information to an existing satellite constellation. Challenges for Cubesat ISL and the digital communication scheme were discussed in [4]. The authors in [5] studied the feasibility of implementing networking transport protocols, Transmission Control Protocol and User Datagram Protocol, in a QB50 Cubesat constellation. The authors in [6] simulated and verified that Cubesats can be used as communication relays for a small fleet of UAVs in an area of operations. In [7], [8], the authors looked into using Cubesats to provide global coverage that minimized the maximum revisit time. The method to obtain global coverage for a LEO satellite network and the necessity of having overlapping footprints were discussed by the authors in [1].

From previous work, we see that the Cubesat constellation is primarily used for observational or surveillance missions that do not require continuous global coverage. The feasibility to employ Cubesat ISL has been proven by past researchers, but the

discussions have been generally restricted to non-continuous global coverage. In this thesis, we build on the previous research findings and propose Cubesat constellations that are capable of providing continuous global coverage.

D. THESIS ORGANIZATION

The thesis consists of five chapters. Cubesat and the various constellation architectures are discussed in Chapter II. Two modes of communication links, namely wireless and optical links, together with modulation techniques, are reviewed in Chapter III. Simulation procedures to determine the coverage of the proposed constellation, trade-off analysis, and link budget analysis are examined in Chapter IV. The conclusion and recommended future work are provided in Chapter V.

II. CUBESAT

Cubesats are gaining popularity in the satellite communications market due to advancements in technologies and miniaturization of low-cost, commercial off-the-shelf (COTS) components. The low cost to deploy a Cubesat in LEO as compared to a mainstream satellite communication system, typically in a geostationary-earth orbit (GEO), is another impetus for the increased usage of Cubesat as a platform for space exploration among research institutes, as funding is more easily achievable. Satellites can also be deployed in the medium-earth orbit (MEO). The various earth orbits available are shown in Figure 3.

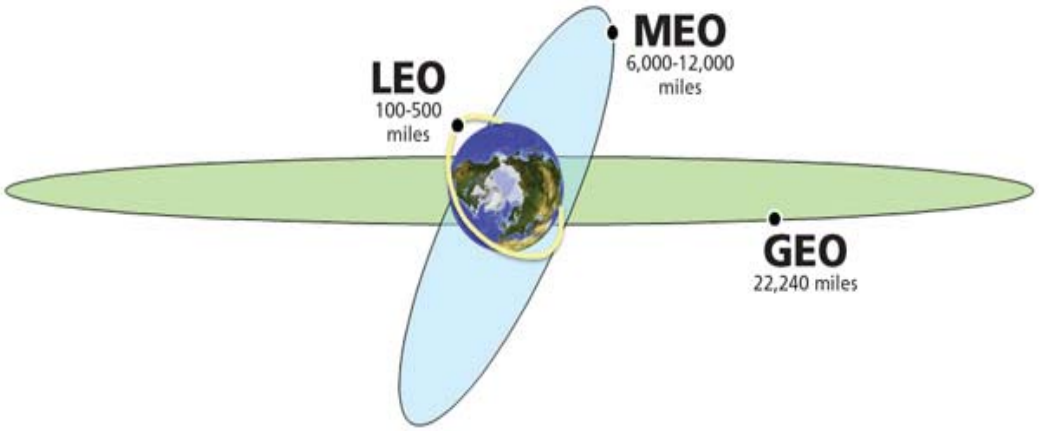

Figure 3. Orbits in Space. Source: [9].

Cubesat was conceived in 1999 through a collaborative effort between Stanford's Space Systems Development Laboratory and California Polytechnic State University's Multidisciplinary Space Technology Laboratory [4]. The aim of the project was to define a standard design specification for a small satellite in order to reduce the design phase and deployment cost and increase access to space through quick launches for space research purposes. The project was so successful that it spearheaded the evolution of numerous low-cost, small satellite deployments.

The launch of Cubesats increased exponentially after the first launch in 2003 [10], with a cumulative total of 424 Cubesat launches by 2015. Cubesat launches peaked in

recent years, with 72.8% of the total launches occurring in the last three years. A graph showing the history of the Cubesats launched per year is shown in Figure 4.

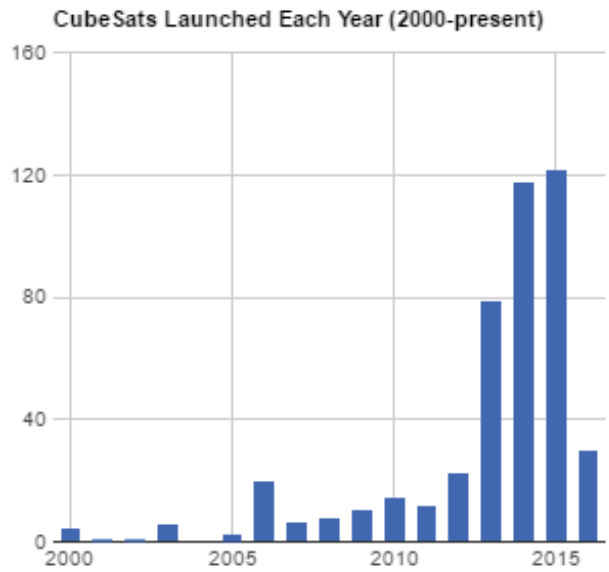

Figure 4. Trends of Increasing Numbers of Cubesats Launched per Year. Source: [11].

The current means of launching a Cubesat is to piggyback on other satellite launches as the secondary payload, and there is no way to specify a particular orbit for the Cubesat [12]. A propulsion system is required to maneuver the Cubesat to its designated orbital position. Being a piggyback payload is both time and fuel inefficient, as the Cubesat mission is dependent on the launch schedule of the primary payload. With an increased demand for Cubesat systems, the National Aeronautics and Space Administration (NASA) is exploring means of having dedicated Cubesat launches. NASA hopes to clear the backlog of 50 Cubesats waiting to be launched [13]. The dedicated launches will also provide the capability to efficiently launch a large number of Cubesats within a short duration.

A. CUBESAT

A Cubesat is a satellite with a structure of 10 cm by 10 cm by 10 cm, weighing approximately 1 kg [14], which is launched into LEO orbit. The Cubesat design frame is

based on a single rack unit (1U) configuration and is scalable to form a 2U and 3U configuration, which represents double rack units and triple rack units, respectively. An example of a 1U Cubesat is shown in Figure 5.

Figure 5. A 1U Cubesat. Source: [15].

There are several classifications of miniature satellites, defined as satellites under 500 kg, depending on the mass of the satellite [16]. A Cubesat is commonly referred to as a picosatellite even though its weight may exceed the typical definition of a picosatellite. The classifications of miniature satellites based on mass are shown in Table 1.

Table 1. Classifications of Miniature Satellites

Classifications	Mass
Minisatellite	100–500 kg
Microsatellite	10–100 kg
Nanosatellite	1–10 kg
Picosatellite	0.1–1 kg
Femtosatellite	0.01–0.1 kg

Similar to a typical satellite design, a Cubesat has a platform structure and a payload. The platform structure comprises the main frame structure for launch and protection, as well as the power subsystem, thermal control subsystem, attitude control subsystem, and data handling subsystem [17]. Different payloads such as repeaters, sensors, and cameras can be deployed, with the payload selection being dependent on the objective of the mission.

1. Advantages of Cubesat

The key advantages of a Cubesat are the low cost and the short time needed to build and deploy a Cubesat. This allows a constellation of Cubesat to be launched quickly and much more cheaply than the launch of a conventional satellite. For example, the cost to launch a single simple Cubesat for research is U.S. $52,000 [18], while the cost to launch a GEO satellite can range from U.S. $50 million to U.S. $400 million [19].

In our mission requirement, we use a UAV as the terrestrial terminal for communication with the Cubesat. Due to the space constraints, the antenna deployed on a UAV is smaller, leading to a lower transmit power. With the Cubesats deployed at a lower altitude, there is less free-space propagation loss as compared to satellites in GEO as the distance from the terrestrial terminal to the Cubesat is much shorter.

By virtue of Cubesat's deployment in a LEO, the propagation delay time is significantly shorter than the delay from a conventional GEO satellite. This allows us to support real-time applications that require short network latencies.

These advantages reinforce the selection of a Cubesat constellation in LEO as the network communication backbone for providing continuous global coverage to the UAVs as the terrestrial receivers.

2. Disadvantages of Cubesat

Although the Cubesat has many advantages, it has some disadvantages worth consideration. Cubesats usually have a short lifespan, ranging from days up to a few years, mainly due to the limitation on the survivability of the COTS components in a space environment. Given the intrinsic nature of a LEO, which has a higher atmospheric density, the Cubesats are vulnerable to experiencing high drag forces. As a result, the Cubesats gradually slow down and are ultimately pulled toward Earth over time [20]. Knowing that the decay rate of a LEO satellite is inversely proportional to its orbital height, we must consider that the lower the Cubesats are deployed, the shorter their lifespan; however, there are also cases where the shorter lifespan is preferred due to operational considerations.

Another disadvantage is the short dwell time of the Cubesat over a designated area due to the high orbital velocity, approximately 26,000 to 27,000 km per hour [21]. The revisit period for the Cubesat is dependent on the orbital design, designated location, and onboard sensor properties [22]; therefore, to achieve continuous global coverage with an increased dwell time and high revisit periods, we require a constellation of Cubesats to be launched.

In a LEO, the coverage footprint of a Cubesat is much smaller due to the fact it is located at a lower attitude. An example of a LEO footprint coverage for various orbital heights and elevation angles is shown in Figure 6.

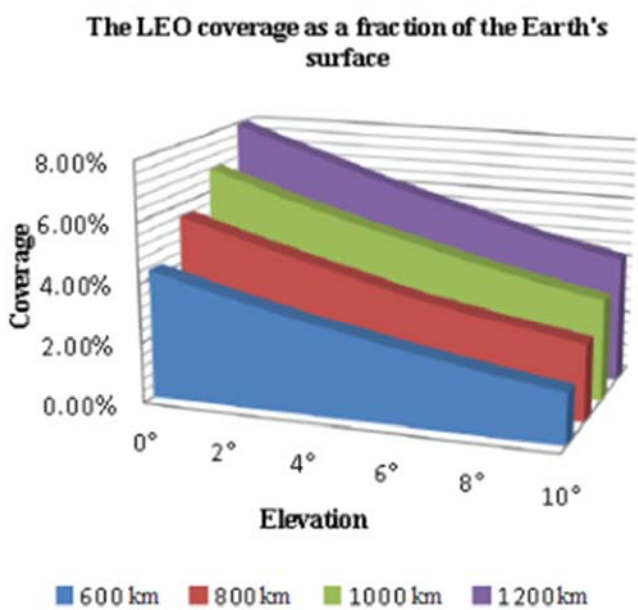

Figure 6. Coverage of Leo Satellites. Source: [1].

We observe that the higher the altitude, the larger the footprint. When compared to satellites in GEO orbit, where three satellites equally spaced are sufficient to provide near global coverage [23], a LEO orbital design requires a constellation ranging from a few hundreds or even thousands of satellites to be deployed to provide the same global coverage. Even with a constellation of Cubesats, there is still a need to employ ISL

techniques between satellites in a constellation in order to achieve real-time data transfer between nodes.

Lastly, owing to size constraints, it is challenging to equip a Cubesat with additional payload components to augment its nominal capability. The Cubesat is also power limited, as the number of batteries and solar powered cells a Cubesat can carry is constrained.

B. SATELLITE CONSTELLATION

Satellite formation flying refers to having a group of satellites that work together to improve the performance of a primary satellite [24]. There are three kinds of satellite flying formations: trailing formations, cluster formations, and constellation formations. In a trailing formation, one satellite follows the preceding satellite along the same orbital path. The trailing formation is best suited for meteorological and environmental applications whereby the area of focus is fixed and there is a need to view the condition of the area at different periods of time. An example of a trailing satellite formation is shown in Figure 7.

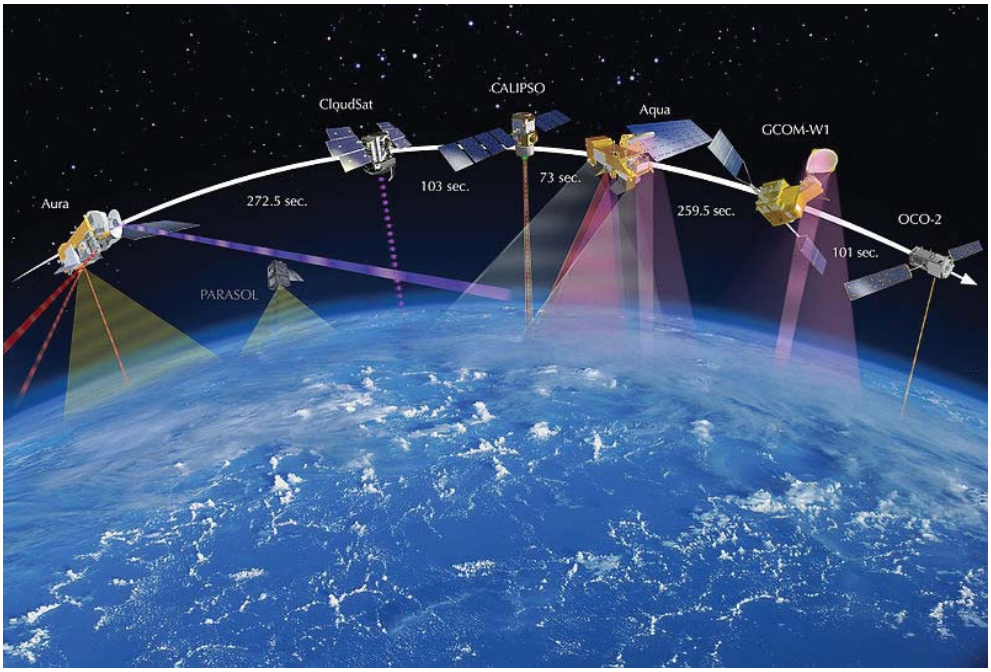

Figure 7. Trailing Satellite Constellation. Source: [25].

Cluster formations refer to a large group of satellites over a designated area. This type of formation is best suited for applications where a localized area-of-operation is the primary focus of the mission.

Constellation formations refer to having a group of satellites with similar properties and common control, deployed in a manner in which each satellite in the constellation compliments the others to enhance the overall coverage area [24]. A single LEO satellite has a limited and moving footprint due to the high velocity the satellite maintains in order to remain in orbit; therefore, we must deploy a constellation of satellites to achieve global coverage.

As both trailing and cluster formations are unable to provide continuous global coverage, our area of focus for this research was on constellation formations.

1. LEO and MEO Constellation

Satellite constellations are primarily deployed in LEO and MEO. Popular applications deployed for MEO constellations are for global positioning systems (GPS). A summary of existing largescale satellite constellations in LEO and MEO and their corresponding status, mission objective, and orbital parameters is given in Table 2.

Table 2. Summary of Satellite Constellations

Constellations	Status	Mission	Orbit	Orbital Height (km)	Inclination (deg)	Constellation Size	Design criteria
Global Positioning System	Deployed	Global navigation	MEO	20,200	55	24	6 planes of 4 satellites
Galileo	Deployed	Global navigation	MEO	23,222	56	30	3 planes of 10 satellites
GLONASS	Deployed	Global navigation	MEO	19,130	64	24	3 planes of 8 satellites
O3B	Deploying	Global Internet	MEO	8000	0	20	To be finalized.
Globalstar	Deployed	Satellite telephony	LEO	1414	52	48	8 planes of 6 satellites
Iridium	Deployed	Satellite telephony	LEO	781	86.4	66	6 planes of 11 satellites
OneWeb	Proposed	Global Internet	LEO	1200	To be finalized.	640	To be finalized.
Teledesic	Previously Proposed	Broadband	LEO	700	98.2	288	12 planes of 24 satellites

OneWeb and Teledesic mission profiles are similar to Cubesat mission requirements; thus, we expect the Cubesat constellation size to be similar to these two missions. Satellite constellations in MEO, such as GPS, Galileo, GLONASS, and O3B require a significantly smaller constellation size.

2. Operational and Developmental Cubesat Constellation

Currently, Flock is the only operational LEO satellite constellation of 3U Cubesats and is dedicated to earth observations [26]. On December 7, 2015, the latest fleet of twelve Flock-2E earth observation (EO) satellites was successfully launched. Designed, manufactured and operated by Planet Labs, Flock 2E is a Cubesat constellation that aims to deliver high resolution images of the earth [27]. The first generation of Flock satellites, Flock-1B and Flock-1C, are operated in the MEO inclination and polar orbits, respectively [28]. A picture of the first two Flock-1 Cubesats being deployed is shown in Figure 8.

Figure 8. Deployment of First Two Flock 1 Cubesats. Source: [26].

There are two more Cubesat constellations in development, namely Lemur-2 and QB50. Lemur-2 is a 3U EO Cubesat operated by Spire for imaging and marine tracking purposes [29]. The first Lemur Cubesat was deployed in 2014 and served as a prototype for a planned design constellation of 100 Cubesats [29]. The QB50 satellite constellation will consist of a network of 50 Cubesats deployed in the lower thermosphere at an

attitude of 200 km to 380 km. The mission of QB50 is for scientific research, educational purposes, technology demonstrations, and access to space [30].

To date, operational Cubesat constellations have been used for observational or surveillance missions. These constellations demonstrate the feasibility of deploying Cubesats at a large scale to perform specific missions. Deploying large scale Cubesat constellations as a network of communication nodes and using them for ISL will undoubtedly be challenging due to their small form factor and power limitations.

3. Designing a Constellation

With the small form factor and power limitations, it is paramount that the satellite constellation be designed in a manner such that the number of satellites deployed is optimized without compromising the fulfillment of the mission requirements. The ultimate satellite constellation design is dependent on parameters such as the orbital height, inclination angle, and separation distance. The main parameters and the corresponding mission impacts to be considered for the design of a satellite constellation are shown in Table 3.

Table 3. Summary of Parameters. Source: [31].

Parameters	Mission Impacts
Number of Satellites	Affects the coverage and the principal cost.
Number of Orbital Planes	Varies based on coverage needs. Highly advantageous to have a minimum number of orbital planes as transfer between the orbits increases the launch and transfer costs.
Minimum Elevation Angle	Must be consistent with all satellites. Determines the coverage of single satellite.
Altitude	Increases the coverage and the launch, transfer cost when altitude is increased. Decreases the number of Satellites. For communication applications, increase/ decrease in altitude can correspondingly change latency.
Inclination	Determines the latitude distribution of coverage and selected based on coverage needs.
Plane Spacing	Results, when plane spacing is uniform, in continuous ground coverage.
Eccentricity	Determines the type of orbit of the satellite.

To date, existing satellite constellations in LEO have been deployed with similar profiles, whereby the satellites operate at the same height, inclination angle, and orbital velocity. The purpose for such a deployment style is to lower the overall deployment cost and enhance ease of implementation. Space engineers also design satellite constellations that require the minimal number of orbital planes and the fewest satellites to meet mission objectives. Moreover, with the same profile, satellites experience similar atmospheric effects and have similar orbital velocities; therefore, the satellites have the same decay rate. This allows the determination of the mission supportable lifespan of the Cubesat constellation; thus, satellites with the same profile are preferred.

4. Constellation Architecture for Global Coverage

There are two common constellation architectures for generating a large number of satellites for global coverage, namely Walker and Street-of-Coverage (SOC). The constellation of satellites using Walker's pattern has the same latitude and inclination; it is also symmetrical. Using Walker's notation, the satellite constellation is defined by the parameters T, P, F and i [32], where T is the total number of satellites in the constellation, P is the number of commonly inclined orbital planes, F is the relative phasing parameter, and i is the common inclination for all satellites. To achieve the symmetry required for Walker's pattern, the satellites in each inclined plane are equally spaced, and the orbital planes are separated equally around the Earth [32]. An example of the Walker pattern is shown in Figure 9.

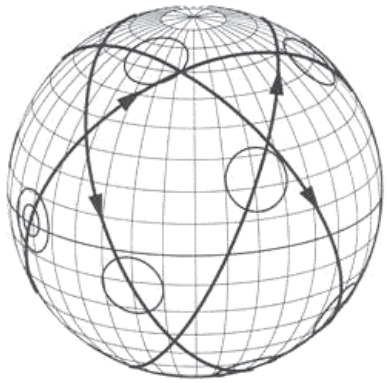

Figure 9. Walker's Constellation. Source: [32].

Based on Walker's concept, the inclination angle constrains the upper and lower latitudinal bound limits of the footprint coverage region, and there is not any coverage at the latitudinal zones beyond the inclination angle. An example of a satellite's path with an inclination angle at 60° is shown in Figure 10. Note that coverage only exists between 60° North and 60° South.

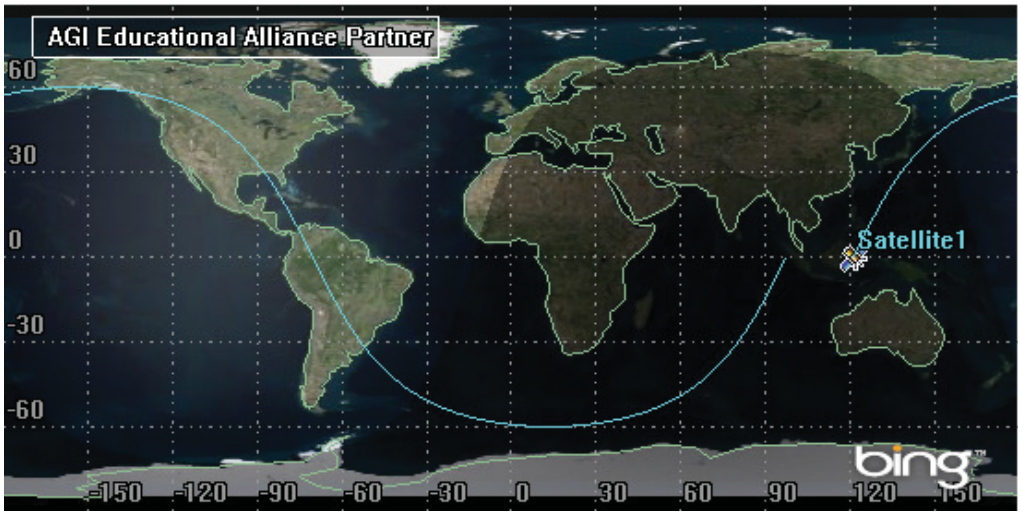

Figure 10. Path of the Satellite with Inclination Angle at 60°

The SOC architecture is based on the concept of having several overlapping, trailing satellite constellations, where the satellites are located at the same altitude and in the same orbital plane. This trail of circular satellite footprints translates to a zone of continuous satellite coverage, termed a street. To obtain global coverage, we need to determine the number of streets required, which is related to the number of orbits needed. An example of the SOC is shown in Figure 11.

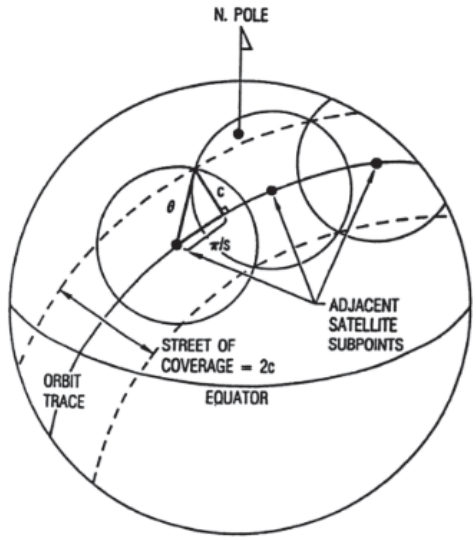

Figure 11. Streets of Coverage. Source: [32].

a. Polar Orbit Constellation Using Walker's Concept

For missions that require continuous global coverage in high-latitude areas or the polar region, we consider using Walker's concept. Having the same satellite profile for all the Cubesats, we see that design and implementation is less complicated and less costly. The trade-off for this concept is poorer coverage over the equatorial region. An example of a polar orbit constellation using the Walker concept is shown in Figure 12.

b. Inclined Orbit Constellation with Modified SOC Concept

For missions that require continuous global coverage with emphasis on the equatorial region or the low latitude zones, we recommend using a modified SOC concept. This is performed by deploying Cubesats at different inclination angles, where the orbital planes are equally spaced over 180°. The trade-off for this design is the longer time needed to deploy the satellite constellation and the need to have multiple launch sites to deploy the satellites into different inclination planes. Moreover, with the satellites deployed into different orbits, the decay lifespan will vary. This phenomenon makes it difficult for continuous sustainment of the satellite constellation as the effort to track and replace the deorbited satellites is significant. An example of an inclined orbit constellation using a modified SOC concept is shown in Figure 13.

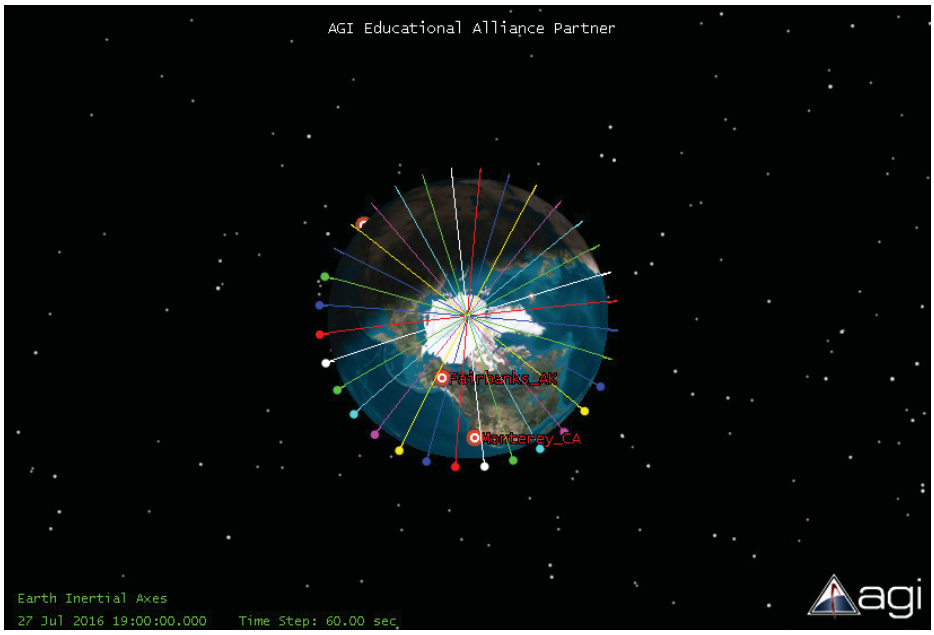

Figure 12. Polar Orbit Constellation

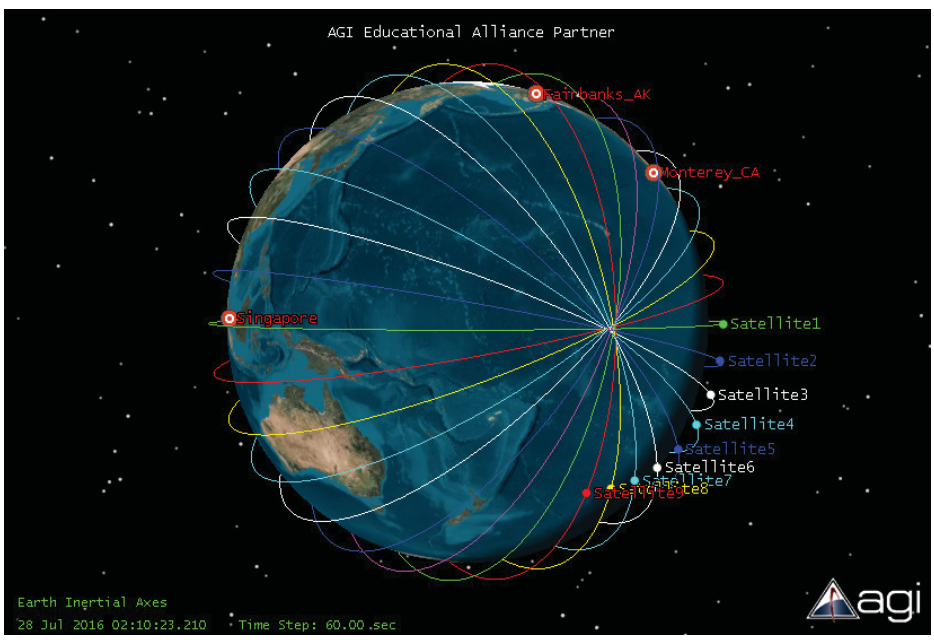

Figure 13. Inclined Orbit Constellation

THIS PAGE INTENTIONALLY LEFT BLANK

III. COMMUNICATION LINK

A communication link is the channel that allows the transmission of information from the source (transmitter) to destination (receiver). Radio frequency (RF) communication has been the de facto mode for satellite communication, and its advantages are widely recognized. Free-space optical communication, though still in its infancy stage, has been extensively researched as well. With the increasing data requirements of modern day applications, the use of optical links that support large bandwidths is of significant interest.

Laser is a form of optical communication, and this technology is frequently studied in the application of ISL. There is great potential for the application of optical communication as it promises numerous advantages over RF communication.

A. MODE OF COMMUNICATION

A comparison of the two modes of communications, RF and optical links, is shown in Table 4.

Table 4. Comparison between RF and Optical Communication. Adapted from [33], [34].

Property	RF Communication	Optical Communication
Data Rate	Lower	Higher
Bandwidth	Lower	Higher
Antenna size	Larger	Smaller
Security	Less secure	More secure
Frequency Spectrum	License required	License free
Cloud Penetration	No effect	Highly vulnerable
Beamwidth	Wide	Highly directive
Acquisition, Tracking and Pointing (ATP) requirement	Less stringent	Highly stringent

In the past few years, there have been several developments in the implementation of optical communication for ISLs, ground-to-satellite links, and deep space missions [34]. NASA's Optical Payload for Lasercomm Science (OPALS) experiment has successfully demonstrated the capability of uploading 175 megabytes of data in 3.5 s using laser communications [35]. The illustration of NASA's OPALS is shown in Figure 14.

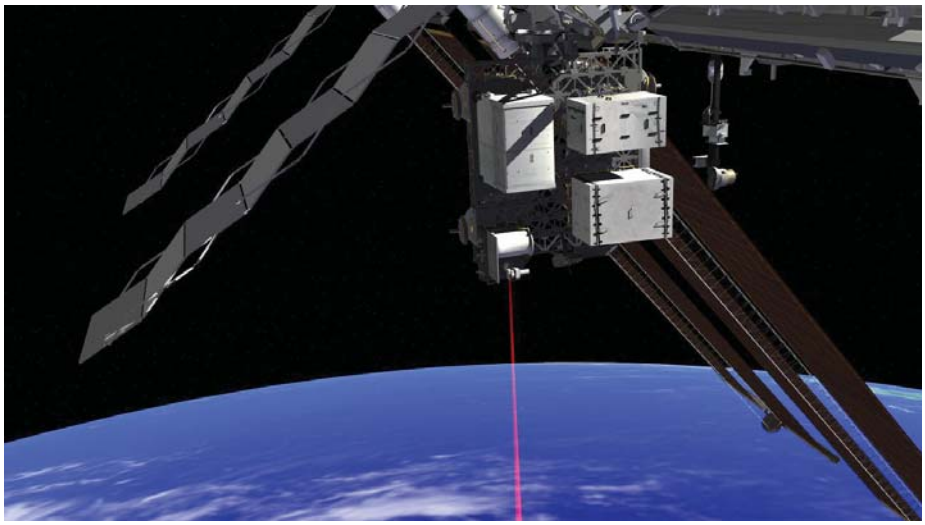

Figure 14. NASA's OPALS Laser Communication. Source: [35].

At present, despite significant development and research in the area of optical links, actual implementation of optical links for Cubesats still poses a huge challenge. Optical links have a short communication range when compared to RF. In addition, the acquisition, tracking, and pointing (ATP) system required for the high precision direction of optical links is still in the research and development phase [36]; therefore, the feasibility of implementing an optical link for Cubesats will only be economically viable when there is a technological breakthrough or proliferation of optical COTS hardware, such as the development of a COTS ATP system. Until then, RF will still be the primary mode of communication for Cubesats.

B. MODULATION TECHNIQUES

Modulation is an important aspect of a communication system as a good modulation technique ensures that information can be correctly received with minimal errors.

In digital communication, modulation is the process of encoding information onto a carrier signal by modifying one or more parameters of the basic carrier signal before it is physically transmitted. These parameters can be amplitude, frequency, or phase [37]. The receiving end must demodulate the signal to extract information from the modulated carrier signal. Two basic digital modulation techniques often used in satellite communication are frequency-shift keying (FSK) and phase-shift keying (PSK). FSK and PSK are modulation techniques whereby data is transmitted through changes in carrier frequency and phase, respectively. Code-shift keying (CSK) is another modulation technique, where data is modulated and transmitted as baseband orthogonal signals.

Binary frequency-shift keying (BFSK) is widely used as the modulation technique for Cubesats due to the ease of allocating designated frequency bands to individual end users; however, it is less power efficient than binary phase-shift key (BPSK). BPSK is a popular technique used due to its properties of power and bandwidth efficiency. Quadrature phase-shift keying (QPSK) is able to achieve twice the spectral efficiency of BPSK while maintaining the same power efficiency; as a result, QPSK is commonly deployed in satellite communication, cellular communication, and wireless communication systems [38]. For power limited applications such as Cubesat, we recommend implementing M-ary orthogonal modulation techniques such as MFSK and MCSK.

The probability of bit error P_b of coherent BFSK is [38]

$$P_b = Q\left(\sqrt{\frac{E_b}{N_0}}\right), \tag{1}$$

where E_b is the average bit energy, N_0 is the one-sided noise power spectral density, and E_b/N_0 is the bit energy-to-noise density ratio.

The probability of bit error of coherent BPSK and QPSK is given by [38]

$$P_b = Q\left(\sqrt{\frac{2E_b}{N_0}}\right), \tag{2}$$

and we see that BFSK requires 3.0 dB more in E_b/N_0 to achieve the same probability of bit error as BPSK and QPSK. That said, the probability of bit error of M-ary phase-shift keying (MPSK) deteriorates as M increases, whereas the converse is true for M-ary frequency-shift keying (MFSK) [38].

The probability of bit error of coherent M-ary CSK (MCSK) and MFSK is expressed as [38]

$$P_b = \frac{M}{2} Q\left(\sqrt{\frac{E_b}{N_0}\log_2 M}\right), \tag{3}$$

where M is the number of distinct M-ary symbols, and E_s is the symbol energy. A comparison of the probability of bit error for the various modulation techniques is shown in Figure 15.

From the graph, we observe that the probability of bit error for both MCSK and MFSK decrease as M increases. Comparing MCSK and MFSK, we prefer MCSK as the system design since MFSK is more complex. An MFSK modulator requires M corresponding pairs of correlators, while a MCSK demodulator requires only one local oscillator. The link budgets calculated in Chapter IV consider BFSK, QPSK, and MCSK, and the modulation technique that can provide the highest bit rate is recommended based on the results obtained.

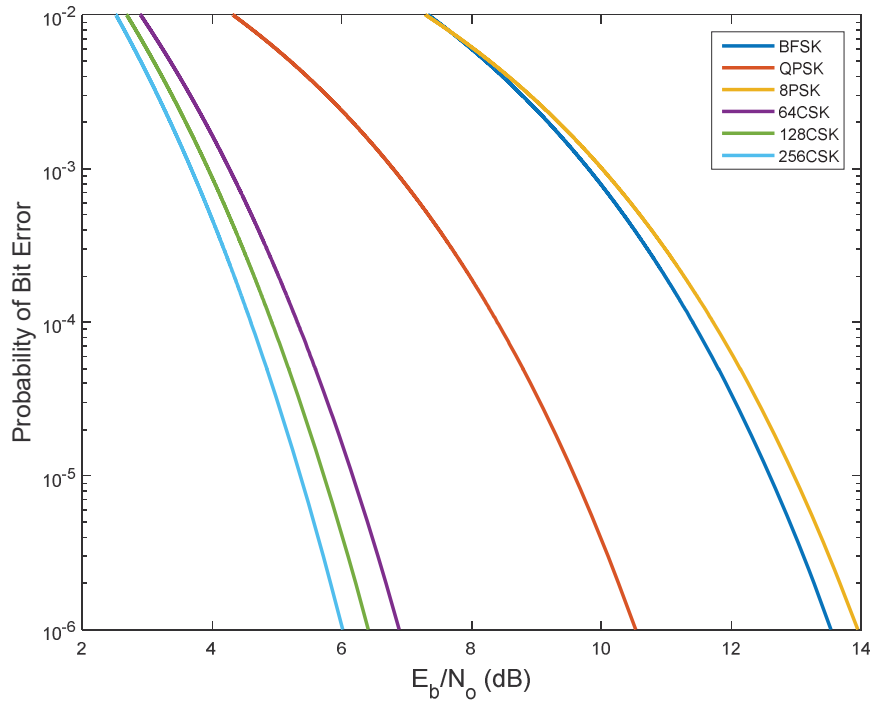

Figure 15. Bit Error Probability for Coherent Modulation Techniques

C. LINK BUDGET

A link budget analysis is the most common form of tool used by communication engineers to verify the link performance and to assess the trade-offs required to close a link. Three different types of links, the uplink from the UAV to the Cubesat, the inter-Cubesat link, and the downlink from the Cubesat to the UAV, are evaluated to determine the feasibility of the communication links. These links are illustrated in Figure 16.

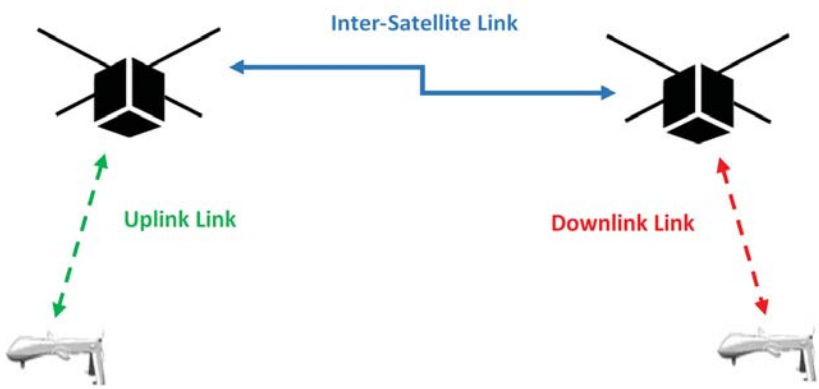

Figure 16. Typical Link Budget Analysis

In the following, the link budget analysis is reviewed using the inter-Cubesat communication link as a reference. The Effective Isotropic Radiated Power (EIRP) of the Cubesat transmitter is [39]

$$EIRP_{dB} = P_{t_{dBW}} + G_{t_{dBi}} - L_{t_{dB}} \ , \tag{4}$$

where P_t is transmitter power of the Cubesat, G_t the transmitter antenna gain, and L_t is other transmitter losses such as cable insertion loss, pointing loss, and etc.

The inter-satellite, free-space path loss L_c is given by the Friis' Transmission formula [39]

$$L_{c_{dB}} = 10\log_{10}\left(\frac{4\pi d}{\lambda}\right)^2 dB \ , \tag{5}$$

where d is the distance between two Cubesat and λ is the signal wavelength. The channel encounters additional losses such as atmospheric absorption, multipath fading, polarization mismatch, and others; thus, the total channel loss L is

$$L_{dB} = L_{c_{dB}} + L_{a_{dB}} + L_{p_{dB}} + L_{o_{dB}} \ , \tag{6}$$

where L_a is atmospheric loss, L_p is polarization loss, and L_o other losses.

The Cubesat received power P_r is

$$P_{r_{dB}} = EIRP_{dB} - L_{dB} + G_{r_{dB}} \ , \tag{7}$$

where G_r is the total receiver antenna gain, inclusive of other receiver losses. For a given bit rate R_b, the energy per bit is defined as

$$E_{b_{dB}} = P_{r_{dB}} - R_{b_{dB}} \ . \tag{8}$$

Next, the Cubesat receiver noise power spectral density is defined as

$$N_{o_{dB}} = \left(kT_{sys}\right)_{dB} \ , \tag{9}$$

where k is Boltzmann's constant and T_{sys} is the receiver system noise temperature. Dividing (8) by (9), we obtain E_b / N_o, and the link margin of the inter-Cubesat link is given by [39]

$$\text{Margin}_{dB} = \left(\frac{E_b}{N_o}\right)_{dB} - \left(\frac{E_b}{N_o}\right)_{\min_{dB}} \ , \tag{10}$$

where $\left(E_b / N_o\right)_{\min}$ is the minimum E_b / N_o to achieve a required bit error probability and is dependent on the modulation technique employed. The same methodology for the link budget analysis is applied to the uplink and downlink paths [40].

The next part of the discussion focuses on the computation of E_b / N_o for multi-hop links, as illustrated in the Figure 17.

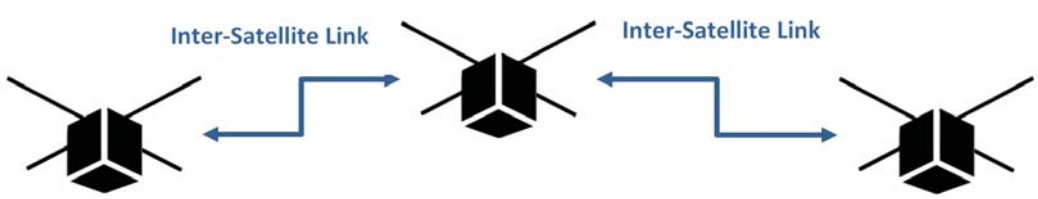

Figure 17. Multi-Hop Link Analysis

Consider the Cubesats as non-regenerative satellite repeaters that operate on the bent pipe principle. Noise from the first link is cascaded to subsequent links, resulting in a deteriorated E_b / N_0. The overall E_b / N_0 for a link consisting of two hops is given by [40]

$$\frac{E_b}{N_0} = \frac{1}{\left(\frac{E_b}{N_0}\right)_1^{-1} + \left(\frac{E_b}{N_0}\right)_2^{-1}} , \tag{11}$$

where $(E_b / N_0)_1$ is the E_b / N_0 of the first hop, and $(E_b / N_0)_2$ is the E_b / N_o of the second hop. As the Cubesats are equally spaced on the constellation, the overall E_b / N_o for a two-hop link on same orbit is 3 dB lower than E_b / N_0 for a single hop.

This calculation can be extended to consider M hops links, whereby the overall E_b / N_o for M hops link is

$$\frac{E_b}{N_o} = \frac{1}{\sum_{i=1}^{M} \left(\frac{E_b}{N_0}\right)_i^{-1}} , \tag{12}$$

where $(E_b / N_0)_i$ is the E_b / N_o of the ith hop; thus, the overall E_b / N_o for an M hop link is $10 log$M dB lower than the E_b / N_0 for a single hop.

As discussed earlier, the physical constraints of a Cubesat result in power-limited satellite; therefore, we recommend that each Cubesat be equipped with an on-board processor so that it can operate as a regenerative satellite repeater with the capability to support multiple hop links, and provide continuous global coverage.

D. NETWORK DELAY

A Cubesat or UAV can be considered as a communication node which is linked via a communication channel to form a network. Latency, or network delay, is a key performance component in satellite communications. Latency can be considered as end-to-end delay, which measures the time required for data or packets to travel from the

source node to the destination node [41]. There are several delay components, such as propagation delay, end-to-end delay, transmission delay, processing delay, and queuing delay.

One of the goals in this thesis was to consider propagation time delay as a factor to determine the optimal separation distance between two Cubesats. The propagation time delay T_{prop} is directly related to the separation distance d between two Cubesat and is defined as

$$T_{prop} = \frac{d}{c} \tag{13}$$

where c is the speed of light in free space.

As discussed in this chapter, Cubesat network deployment must consider the market technology trend, modulation technique to be implemented, link budget analysis, and link latency for mission success.

THIS PAGE INTENTIONALLY LEFT BLANK

IV. PERFORMANCE EVALUATION

In this chapter, the proposed Cubesat constellation architecture needed to meet different mission requirements is stimulated using Systems Tool Kit (STK). STK is a commercial software product available from Analytical Graphics Inc. that is widely used by satellite engineers and developers to model complicated networked systems on the ground and in space. STK is a very powerful tool that allows satellite engineers to easily analyze and visualize results obtained from the simulation. With the aid of STK, the proposed constellation for the various missions in this thesis is determined. The detailed link budget analysis, primarily focusing on the inter-Cubesat links, and modulation techniques to improve the data rate, are also discussed in this chapter.

A. PROPERTIES OF STK SIMULATOR

The key functionality and properties of STK that are used in this thesis are briefly described in this section. First, we need to determine the STK objects required for the simulation.

As shown in Figure 18, we create various scenario objects for our simulation such as satellites, ground stations, and UAVs. The properties of each object can easily be configured. To establish a realistic stimulation, there is also a need to attach sensors or antennas to the objects in order to establish an LOS between the objects.

To configure a Cubesat, we insert its orbital height and the inclination in the orbit wizard as shown in Figure 19. Alternatively, we can use the 'Define Properties' option, which provides more fields to configure the satellite. This inserted satellite is the seed satellite that is subsequently used to create a Cubesat constellation. In this thesis, we primarily focus on circular orbits for the Cubesat constellation.

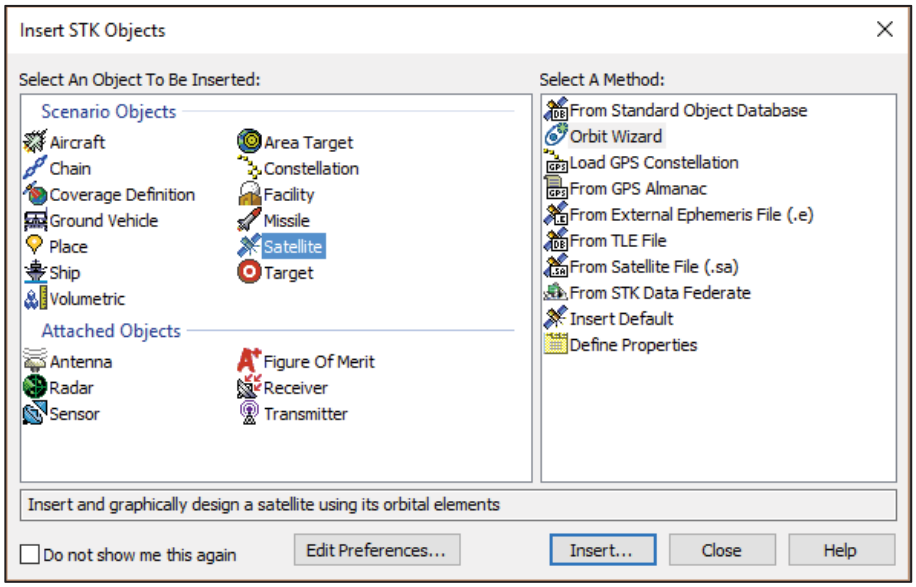

Figure 18. STK Objects

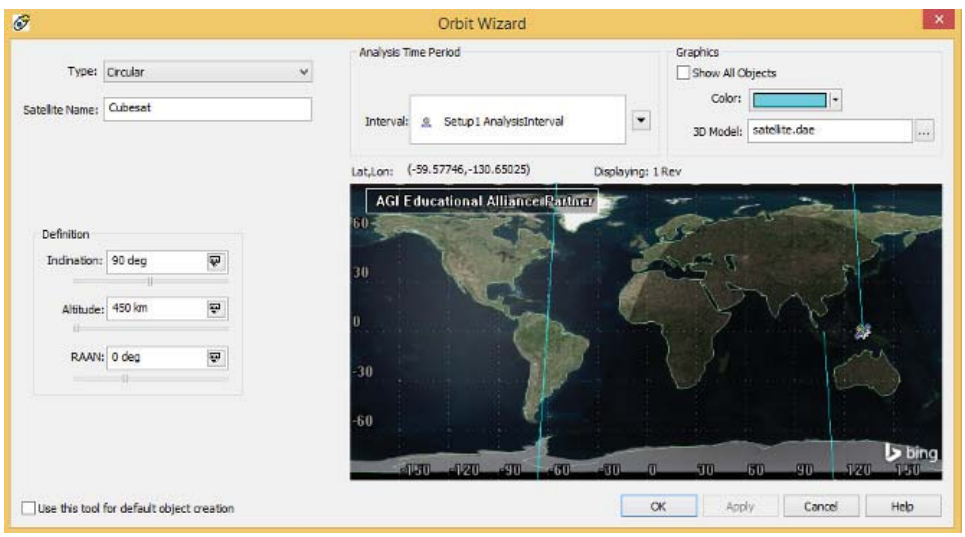

Figure 19. Configure Cubesat Orbital Parameters

We make use of the Walker tool built into STK to create Cubesats on single and multiple planes. The Walker's constellation is selected since it is most symmetrical and the angular phase separation distance between the satellites can be automatically generated. The Walker tool used to create the Cubesat constellation and a pictorial view of the outcome of the designed constellation are shown in Figure 20 and Figure 21, respectively.

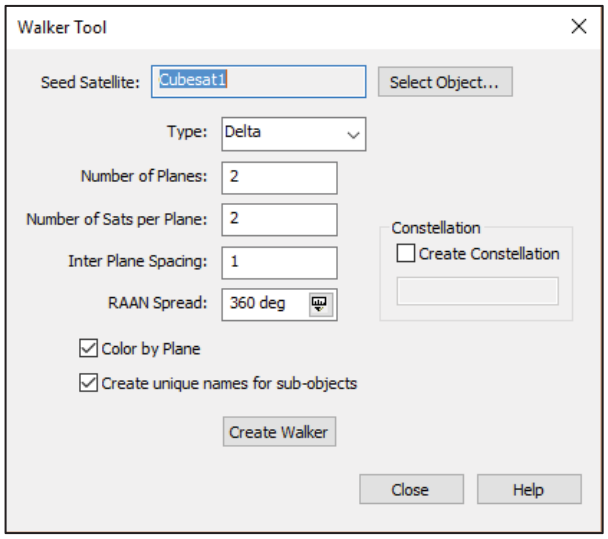

Figure 20. Create Cubesat Constellation

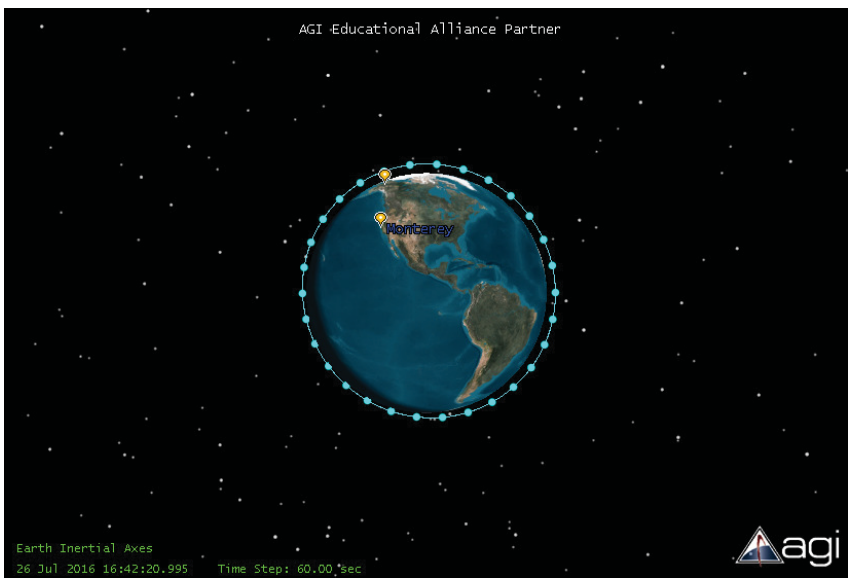

Figure 21. Example of Cubesat Constellation

B. SIMULATION SCENARIOS

(1) Determination of Orbital Height and Collision Avoidance

Collision avoidance is a critical factor to consider in any space deployment. There are two key types of space collisions, namely collision with space debris and collision with existing satellites. With the increasing amount of space debris and congestion of

satellites in LEO, it is important to ensure that the orbital attitude of the deployed Cubesats is free from debris. Collisions render the affected orbital slot useless.

A representation of the existing LEO satellite population is plotted in Figure 22. A majority of satellite collisions occur in sun synchronous orbits at inclinations of 98° and 82° with an orbital height of 480 km to 1100 km [42]. A suitable range for the deployment of Cubesats was determined to be an orbital height from 200 km to 450 km as it is less populated and lowers the risk of collision.

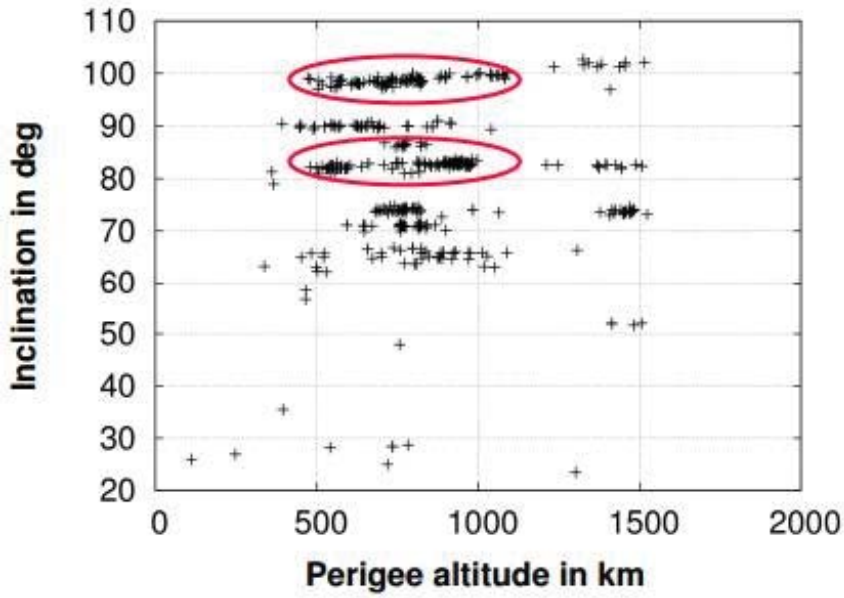

Figure 22. LEO Satellites Population. Source: [42].

The number of satellites or space debris that is trackable, specifically those that have a size that is larger than 1.0 cm, is shown in Figure 23. The most space debris lies in the range of 700 km to 1000 km, and the amount of debris increases each year. This data further reinforces the selection of the orbital height at 200 to 450 km, whereby the probability of collision with both existing satellites and space debris is remote.

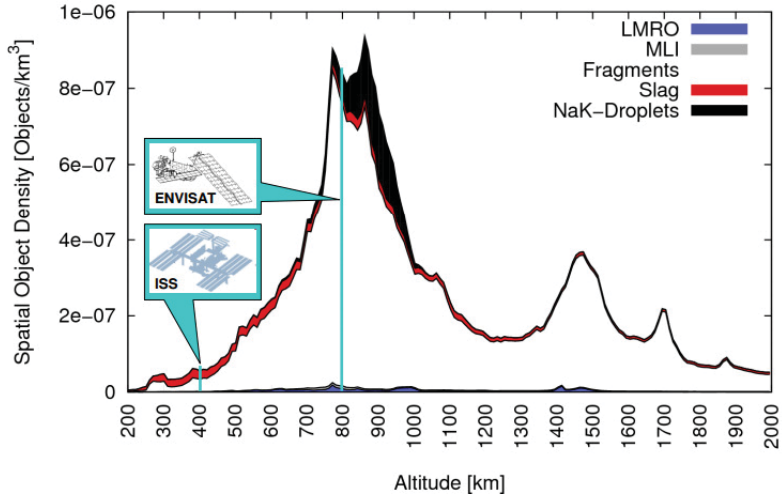

Figure 23. Spatial Density in LEO Orbit. Source: [42].

Collision avoidance between Cubesats in their own constellation also has to be considered. The Cubesat has to stay within an operational box to prevent collisions, and it is also recommended that a combined analysis be performed with neighboring satellite service providers to ensure that every satellite is operating within its design specifications. Conjunction is a term used to refer to a situation whereby a space object is approaching the operation box at a close distance.

Currently, space engineers conduct conjunction analysis for LEO satellites with a 25 km x 25 km x 2 km box [43]. The International Space Station has more stringent requirements whereby maneuvers are performed when space objects come close to the operation box of 25 km x 25 km x 0.75 km for orbits at the attitude between 330 km to 435 km [44]. Based on these examples, we propose that the separation distance for each Cubesat in its own constellation be at least 25 km.

In the Cubesat constellation, there is a convergence and divergence region. The convergence region is either the equatorial or the polar region depending on the constellation design. As the Cubesats are highly concentrated at the convergence region, there is a need to maintain a minimum separation distance between the Cubesats for collision avoidance. Conversely, the divergence region refers to areas where the Cubesats are located the furthest apart.

(2) Decay Lifetime and Corresponding Orbital Height Selection

The decay lifetime of all satellites is dependent on numerous variables, such as the drag force, solar flux, orbit configuration, satellite mass, drag coefficient, and cross-velocity area [45]. As a result, the decay lifetime of a Cubesat is highly variable, and there are many models on the market to perform the predictions. The Jacchia 1971 model is widely used to represent the atmospheric density [32]. We use that model in STK to generate the decay lifetime of a Cubesat starting from 180 km, which is the minimum height for a LEO satellite. The steps to simulate the decay lifetime of Cubesat in STK are shown in Appendix A. The results are verified with statistics acquired through the open literature [45], [46]. A summary of the decay lifetime is shown in Table 5.

Based on stimulated results and considering the standard guideline that limits the lifespan for small satellites to 25 years [47], the maximum orbital height of the Cubesat must not exceed 640 km. The analysis also showed that the ideal orbital height is 450 km as the decay lifetime coincides with the lifespan of typical electronic components and offers a reasonable time frame for the mission. If mission requirements call for short durations, orbital heights from 200 km to 300 km can be considered.

Table 5. Decay Lifetime of Cubesat

Orbital Height (km)	**Decay Lifetime from STK**	**Decay Lifetime Adapted from [45]**	**Decay Lifetime Adapted from [46]**
180	< 1 day	<2 days	-
200	1–3 days	2 days	-
250	7–14 days	5 days	-
300	28–49 days	18 days	29 days
350	81– 158 days	58 days	-
400	155 days –1.5 years	167 days	256 days
450	2.6 – 5.1 years	1.1 years	-
500	1.3 – 7.4 years	2.4 years	4 years
550	268 days – 11.8 years	7 years	-
600	6.2 – 22.5 years	15.1 years	20 years
640	>25 years	>25 years	-

(3) Number of Planes and Number of Satellites per Plane

The methodology to obtain the optimal number of satellites per plane and the number of planes is described in the following section. The illustration of the geometry of a satellite with respect to the Earth is shown in Figure 24.

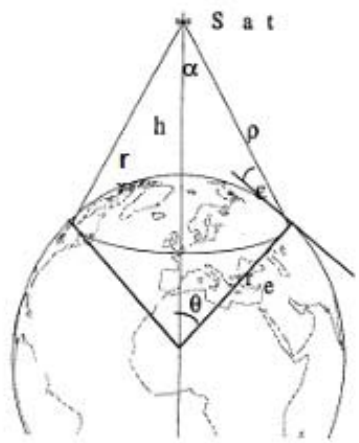

Figure 24. Viewing Geometry of a Satellite. Source: [32].

From this geometry, we first determine the footprint of the Cubesat, or the satellite coverage radius on Earth's surface; the coverage radius r is given by

$$r = h \tan \alpha \tag{14}$$

where h is the satellite orbital height and α is the satellite's field-of-view angle. The Earth's central angle of coverage θ is expressed as

$$\theta = \frac{360}{2\pi} \sin^{-1}\left(\frac{r}{r_e}\right) \simeq \frac{360r}{2\pi r_e},\ r \ll r_e \ \left(\text{degrees}\right) \tag{15}$$

where r_e is the radius of the Earth. We obtain the number of non-overlapping satellite footprints per plane with the expression $360^{\circ}/(2\theta)$. For the purpose of the analysis, we assumed a 20% and 25% increase in the additional Cubesat footprints required to achieve the overlapping coverage. This assumption is verified in the STK simulations. As

Cubesat launches are dependent on p-pods that have been designed to have three Cubesats per pod [48], the number of Cubesats per plane is in multiples of three.

Lastly, as the number of planes is equally distributed around the Earth's hemisphere, i.e., half the Earth's circumference, the number of planes can be expressed as $180^{\circ}/(2\theta)$. Similarly, for the purpose of the analysis, the same assumption of a 20% to 25% increase in the number of planes to achieve the overlapping coverage is applied. The parameters in Table 6 are used in the simulations to determine the selection of the Cubesat constellation deployment in the next section.

Table 6. Proposed Parameters for STK Simulation

Orbital Height (km)	Footprint Radius of Cubesat (km)	Number of non-overlapping Cubesats per plane	Number of overlapping Cubesats per plane		Proposed number of Cubesats per plane	Proposed number of planes
			20%	25%		
450	779	26	31	32	30, 33	15, 16, 17
300	520	39	46	48	45, 48	22, 23, 24
200	346	58	69	72	69, 72	34, 35, 36

(4) Coverage of the Constellation

Coverage is defined by the duration where there is LOS between the Cubesat and ground station or the time that the ground station has access to at least one satellite. As the footprint of each Cubesat overlaps the oncoming Cubesat, the ground station always has continuous coverage; i.e., there is a handshake from one Cubesat to another. For locations not in the desired area-of-interest, there are intermittent periods when there is no coverage as the LOS with the Cubesat is lost; however, the next coverage period commences once LOS is established with the Cubesat from the next nearest plane.

Coverage of a location is the key consideration when determining the optimal Cubesat constellation; thus, we have selected three locations, Singapore, Monterey, and Fairbanks, with varying latitudes to determine the constellation coverage. Singapore, at a latitude of 1.29°, represents the coverage at the equatorial region. Monterey, at a latitude of 36.60°, is ideally located to represent coverage in the median latitude region. Lastly,

Fairbanks, at a latitude of 64.84°, which is close to the Arctic Circle (66.57°), is selected as it provides a good representation of the coverage in the polar region. An overview of the locations selected is shown in Figure 25.

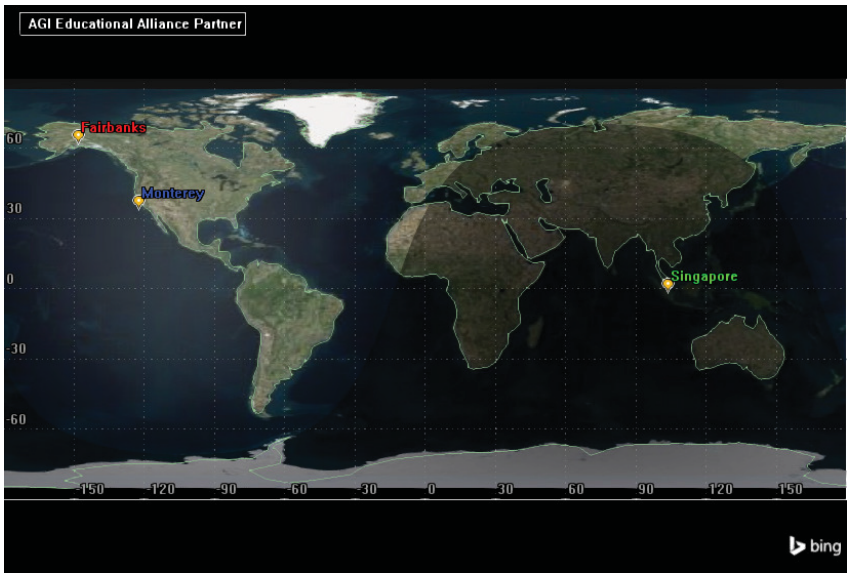

Figure 25. Locations Selected for Stimulation

After these locations are inserted into STK, we proceed to insert the Cubesat. We utilize the Walker tool to generate the constellations required for simulation. Sensors need to be attached to each satellite to emulate the Cubesat's field-of-view and its footprint. We configure the sensor type as 'Simple Conic' and set the cone half-angle to be 60°. This angle is the practical beamwidth of a Cubesat omni antenna. A representation of a ring of footprints generated by the Cubesat constellation on a single plane is shown in Figure 26. The steps to simulate the coverage of the Cubesat constellation in STK is shown in Appendix B.

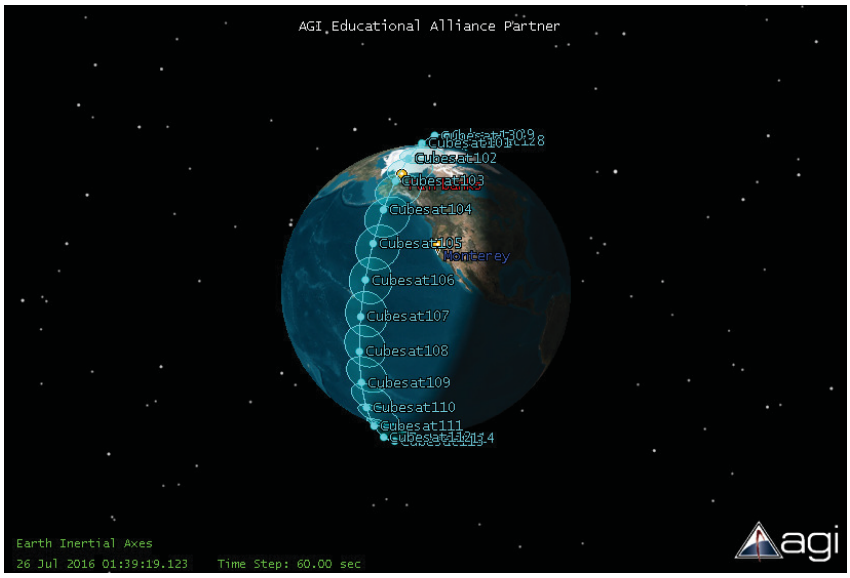

Figure 26. Footprint Generated by a Cubesat Constellation

An example of a polar constellation configuration with multiple planes to achieve continuous global coverage generated through STK is shown in Figure 27.

Figure 27. Polar Constellation of 17 Planes with 33 Satellites per Plane

A final example of an inclined constellation configuration that is used in the simulation scenarios is shown in Figure 28.

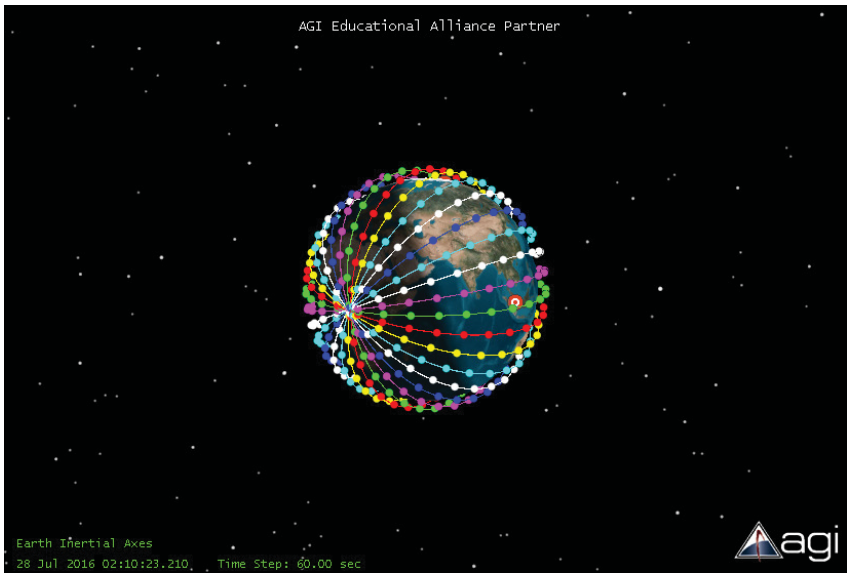

Figure 28. Inclined Constellation of 16 Planes with 30 Satellites per Plane

C. PROPOSED CUBESAT DESIGN CONSTELLATION

The criteria for selection of the Cubesat constellation are dependent on the link availability, desired area of operation, and duration of mission. Simulations based on the proposed orbital heights of 450 km, 300 km, and 200 km are performed. The aim of the simulation is to determine the optimal Cubesat constellation configuration with high link availability, a mission supportable lifespan, and collision avoidance.

For the purpose of the analysis, mission requirements for link availabilities have been defined to be 99.9% for good coverage at the convergence point, at least 95% coverage for the median latitude region, and a minimum of 90% coverage for the diverged region. The simulation results for orbital heights of 450 km, 300 km and 200 km are shown in Table 7, Table 8 and Table 9, respectively.

Table 7. Simulation Result for Orbit Height of 450 km

Orbital Height	Type of Orbit	Lifetime from STK	No. of planes	No. of Sat Per Plane	Total Sat	Sat Separation (km)	Availability (%)		
							Singapore	Monterey	Fairbanks
450 km	Polar Walker	5.1 years	16	30	480	89.378	82.58	91.42	100
			16	33	528	81.253	87.76	96.09	100
			17	30	510	84.121	85.03	92.71	100
			17	**33**	**561**	**76.473**	**90.34**	**97.21**	**100**
			18	30	540	79.447	87.14	93.72	100
	Inclined SOC	2.6 – 5.1 years	14	33	462	92.861	100	97.37	88.52
			15	33	495	86.670	100	96.73	84.15
			16	30	480	89.378	98.25	90.7	91.85
			16	**33**	**528**	**81.253**	**100**	**95.41**	**96.15**
			17	33	561	76.473	100	94.59	95.15

The results of the simulation at the orbital height of 450 km in Table 7 show that a deployment of 33 satellites per plane, with 17 planes in the constellation, provides the optimal result for a polar Walker orbit. Fairbanks, located at the convergent point in this configuration, has a link availability of 100%, while Singapore, being at the most diverged region, achieved the minimum required link availability. Monterey exceeds the link performance requirement for the median latitude region with a coverage of 97.21%.

We also see that a deployment of 33 satellites per plane with 16 planes in a constellation provides the optimal result for inclined SOC orbit. For this orbit type, the convergence point is observed to be in Singapore, which was the most diverged region with the polar Walker orbit. As for the Walker orbit, the convergence point has the best availability.

For this orbit, we observe that the system lifetime for the inclined configuration ranges from a lower threshold of 2.6 years to 5.1 years. The reduction in the lifetime is inherent in the design of an inclined orbit as the inclination angle of the orbit affects the decay lifetime; thus, a polar Walker orbit has the maximum decay lifetime with the inclination angle of 90°.

Both Cubesat constellation configurations far exceed the minimum separation distance required, and this reduces the likelihood of collision.

Table 8. Simulation Result for Orbit Height of 300 km

Orbital Height	Type of Orbit	Lifetime from STK	No. of planes	No. of Sat Per Plane	Total Sat	Sat Separation (km)	Availability (%)		
							Singapore	Monterey	Fairbanks
300 km	Polar Walker	49 days	24	45	1080	38.851	87.34	95.48	100
			24	**48**	**1152**	**36.423**	**90.39**	**97.64**	**100**
			25	45	1125	37.297	88.98	96.2	100
			25	48	1200	34.966	92.01	98.25	100
	Inclined SOC	28-49 days	22	48	1056	39.734	100	92.04	95.03
			24	45	1080	38.851	99.89	98.49	94.91
			24	**48**	**1152**	**36.423**	**100**	**99.4**	**97.33**

At the orbital height of 300 km, we observe that the constellation design of 48 satellites per plane with 24 planes provides the optimal performance result for both types of orbits. At a lower altitude, the total number of satellites needed to achieve similar performance at 450 km nearly doubles. The orbital lifetime is also reduced significantly, with a maximum of 49 days for a polar orbit. Nonetheless, despite the large number of Cubesats deployed, the separation distance still meets the minimum requirement for collision avoidance.

Table 9. Simulation Result for Orbit Height of 200 km

Orbital Height	Type of Orbit	Lifetime from STK	No. of planes	No. of Sat Per Plane	Total Sat	Sat Separation <2 layers> (km)	Availability (%)		
							Singapore	Monterey	Fairbanks
200 km	Polar Walker	3 days	34	69	2346	35.235	88.92	97.48	100
			34	**72**	**2448**	**33.767**	**90.64**	**98.48**	**100**
			35	69	2415	34.228	90	97.87	100
			35	72	2520	32.802	91.83	98.83	100
	Inclined SOC	1 -3 days	32	69	2208	37.437	99.57	93.2	92.97
			32	72	2304	35.877	100	93.96	94.14
			34	**72**	**2448**	**33.767**	**100**	**99.24**	**97.73**

The same approach for orbital heights at 450 km and 300 km cannot be used for analysis at 200 km as the minimum separation distance is calculated to be 16 km, which is less than the minimum separation distance of 25 km needed for collision avoidance. As a result, we need to implement a two-layer constellation design whereby each alternating adjacent plane is staggered in height by 5.0 km. For example, the first plane is located at

an orbital height of 200 km, the second plane is staggered at a height of 205 km, the third plane returns to 200 km, and the fourth plane is again staggered at 205 km. This layering design continues through the last plane. With this approach, we can achieve the minimum required separation distance.

Comparing all three scenarios, we recommend the Cubesat constellation configuration at the orbital height of 450 km. The constellation design at 450 km requires the least number of satellites to achieve both the required link performance and collision avoidance while having the longest decay lifespan. The simulations did show that the other two orbital heights were able to achieve both the required link performance and collision avoidance; however, the number of satellites required increased significantly with the decrease in orbital height. The constellation design with the layering approach at 200 km is the least ideal. With different orbital heights, the Cubesats are traveling at different speeds, and the Doppler effect must be taken into consideration.

D. LINK BUDGET ANALYSIS

To investigate the feasibility of the proposed constellation design, we need to look at the link budget analysis of inter-Cubesat links at the proposed orbital heights. The frequencies of 435 MHz is used for the inter-Cubesat links, 440 MHz for the uplink path, and 430 MHz for the downlink path. The typical modulation technique of Cubesat communication is based on BFSK. We also discuss other modulation techniques to improve the link margin and perform a trade-off analysis. Lastly, we study the link budget analysis for the uplink and downlink paths for the recommended orbital height in order to have a holistic view of the node-to-node communication link using Cubesat as the backbone architecture.

From this analysis, we identify suitable COTS communication components that are currently available in the market for both the Cubesat and UAV systems. Some technical parameters of the proposed constellation, such as the antenna gain, power, and loss are referenced from the identified product specifications and used in the link budget analysis.

The AX100, UHF transceiver from GomSpace was proposed for both the inter-Cubesat links and downlink to the ground receivers, while TRX-U, UHF transceiver from Space Quest was used for the uplink path from the UAV to the Cubesat. The AX100 is only capable of providing a transmit power up to 1.0 W due to its physical constraints. The AX100 also has the matching output power needed, supports a high bit rate, and has better receiver sensitivity than TRX-U transceiver. Knowing that UAV systems have fewer physical constraints and are capable of housing a larger power module, we selected the TRX-U transceiver due to its ability to provide up to 6.0 W of power, improving the link budget. A picture of the AX100 transceiver and TRX-U transceiver are shown in Figure 29 and Figure 30, respectively. The transceiver specifications are shown in Table 10.

Figure 29. AX100 Transceiver for Cubesat. Source: [49].

Figure 30. TRX-U Transceiver. Source: [50].

Table 10. Transceiver Specifications

Links	Component	Frequency Range [MHz]	Transmit Power [dBm]	Date Rate [kbps]	Modulation	Receiver Sensitivity [dBm]
Inter-Cubesat Link, Downlink	GomSpace AX100	395 to 440	30	0.1 to 115.2	FSK,MSK, GFSK,GMSK	-132 at 600 baud -122 at 5 k baud -111 at 50 k baud
Uplink	SpaceQuest TRX-U	370 to 470	30-37.8	2.4 to 19.2	FSK,GFSK	-120 at 2.4 kbps -111 at 19.2 kbps

The NanoCom ANT430 antenna, an isotropic antenna from Gomspace, is used as the antenna for the uplink, downlink and inter-Cubesat links. This antenna has a maximum gain of 1.5 dBi and an average gain of 0.6 dBi. An average insertion loss of 1.0 dB is expected. The diagram and the specifications of ANT430 antenna are shown in Figure 31 and Table 11, respectively.

Figure 31. ANT430 Antenna. Source: [49].

Table 11. Antenna Specifications

Links	Component	Frequency Range [MHz]	Antenna Gain [dBi]	Insertion Loss [dB]
Uplink, Inter-Cubesat Link, Downlink	GomSpace ANT430	400 to 450	-1.0 to 1.5	1.0

With the technical parameters available, we proceeded to investigate the link margin for inter-Cubesat link at the proposed orbital heights of 200 km, 300 km and 450 km. The modulation technique used was BFSK with a bit rate of 9600 bps.

1. Investigating the Link Margin for Inter-Cubesat Link

From the link budget analysis, we observed that there was sufficient link margin for all links at the proposed orbital heights, including the link at the highest proposed orbital height of 450 km, which resulted in the longest inter-Cubesat separation distance. The results of the link budget computation for the inter-Cubesat link for the three different orbital heights are shown in Table 12.

Table 12. Link Margin of Inter-Cubesat Link

Parameter	**Units**	**Link 1 @ 200 km**	**Link 2 @ 300 km**	**Link 3 @ 450 km**	**Remark**
Transmitter Power	dBW	0	0	0	1.0 W power
Transmitter Antenna Gain	dBi	0.6	0.6	0.6	0.6 dBi Omnidirectional Antenna Gain
Transmitter Antenna Losses	dB	1	1	1	Insertion loss
ERIP	dBW	-0.4	-0.4	-0.4	
Free Space Loss	dB	140.89	144.04	147.76	
Atmospheric Loss	dB	0	0	0	Assume negligible loss
Polarization Loss	dB	3	3	3	Circular polarization loss
Other Loss	dB	0	0	0	Assume no loss
Total Loss	dB	143.89	147.04	150.76	
Receiver Antenna Gain	dBi	0.6	0.6	0.6	0.6 dBi Omnidirectional Antenna Gain
Receiver Antenna Losses	dB	1	1	1	Insertion loss
Total Antenna Gain	dBW	-0.4	-0.4	-0.4	
Total Received Power	dB	-144.69	-147.84	-151.56	
Bit Rate	bps	9,600	9,600	9,600	
Bit Rate	dB	39.82	39.82	39.82	
Energy per bit	dB	-184.51	-187.67	-191.38	
Receiver Noise Power Spectral	dB	-202.69	-202.69	-202.69	
EB/No Computed	dB	18.18	15.02	11.31	
Eb/No Required	dB	13.54	13.54	13.54	Using BFSK with P_b of 1e-6
Coding Gain	dB	6	6	6	
Link Margin Required	dB	3	3	3	
Excess Link Margin	**dB**	**7.64**	**4.48**	**0.77**	

Besides achieving the link margin required, we observe that there is an excess link margin based on the analysis. With the excess link margin, we can perform a trade-off analysis using MATLAB to determine how to optimize the link performance. The MATLAB simulation codes to obtain the graphs from Figure 32 to Figure 39 are shown in Appendix C.

We repeated the link budget for different orbital heights by using the excess link margin to reduce the transmit power needed to achieve the minimum link margin of 3.0 dB. As the solar cells on the Cubesats have a limited capacity, the power savings from reduced transmit power can be redistributed to other subsystems on the satellite. The minimum transmit power for each orbital height is shown in Figure 32.

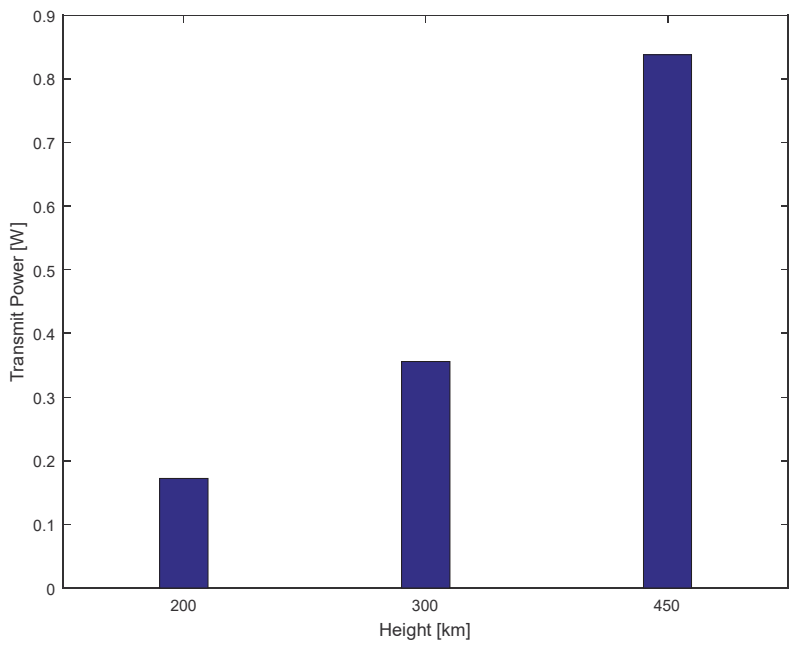

Figure 32. Minimum Transmit Power versus Each Orbital Height

We also investigated the use of the excess link margin to improve the bit rate in lieu of reducing transmit power. The bit rate is improved from 9.6 kbps to 55.76 kbps, 26.96 kbps and 11.46 kbps for the orbital heights of 200 km, 300 km and 450 km, respectively. Focusing on the recommended orbital height of 450 km, we find that the bit

rate of 11.46 kbps is still low. As a result, we must explore other modulation techniques to improve the bit rate. The maximum bit rate for each orbital height is plotted in Figure 33.

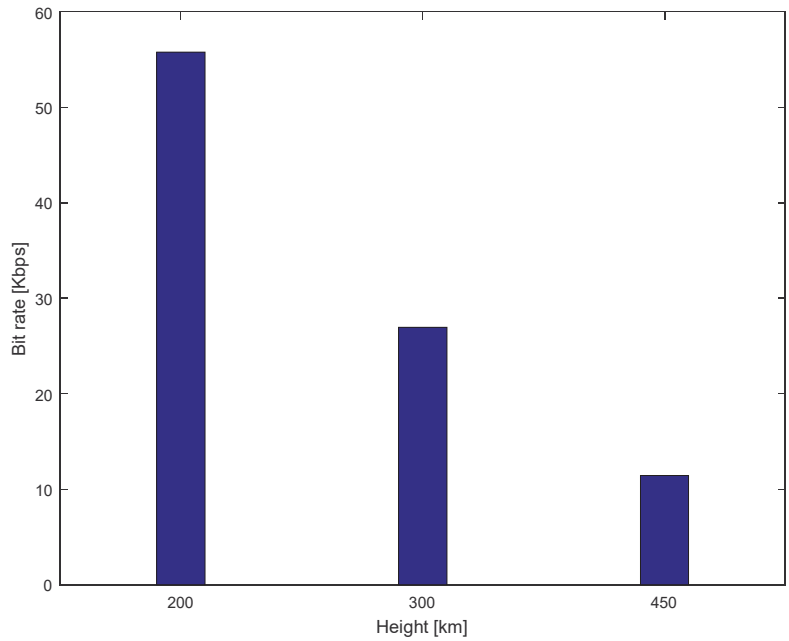

Figure 33. Maximum Bit Rate for Each Orbital Height

In our earlier analysis, we found that although BFSK is the most commonly used modulation technique for Cubesat, it only provides an excess link margin of 0.77 dB. With QPSK, the excess link margin achieved increased but was only 3.78 dB; thus, for power limited applications such as Cubesat, M-ary orthogonal modulation techniques such as code-shift keying can be implemented [38]. With M-ary orthogonal modulation, we observe that the link margin improves significantly, ranging from 7.0 dB to 8.0 dB as the coding changes from 64-CSK to 256-CSK. The link margin for different modulation techniques and the minimum transmit power required for each are shown in Figure 34 and Figure 35, respectively.

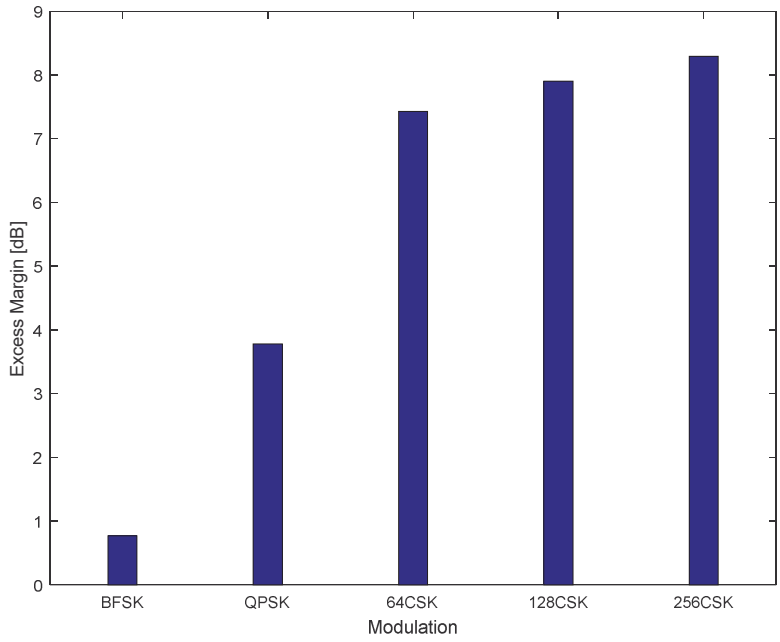

Figure 34. Link Margin for Different Modulation Techniques

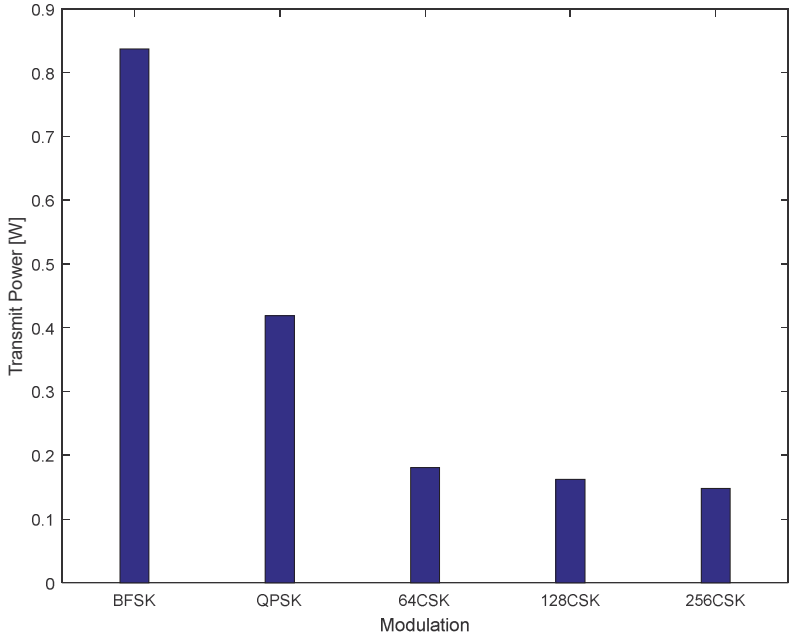

Figure 35. Minimum Transmit Power for Different Modulation Techniques

2. Investigating the Modulation Technique to Achieve Higher Bit Rate

The link budget analysis is repeated to determine the maximum bit rate for different modulation techniques. To achieve a balance between the complexity of the chipset and the bit rate, we recommend that 128 CSK be used. With 128-CSK, we achieve a bit rate of 59.2 kbps, which can comfortably support a 56 kbps inter-Cubesat link. The maximum bit rate for different modulation techniques is shown in Figure 36.

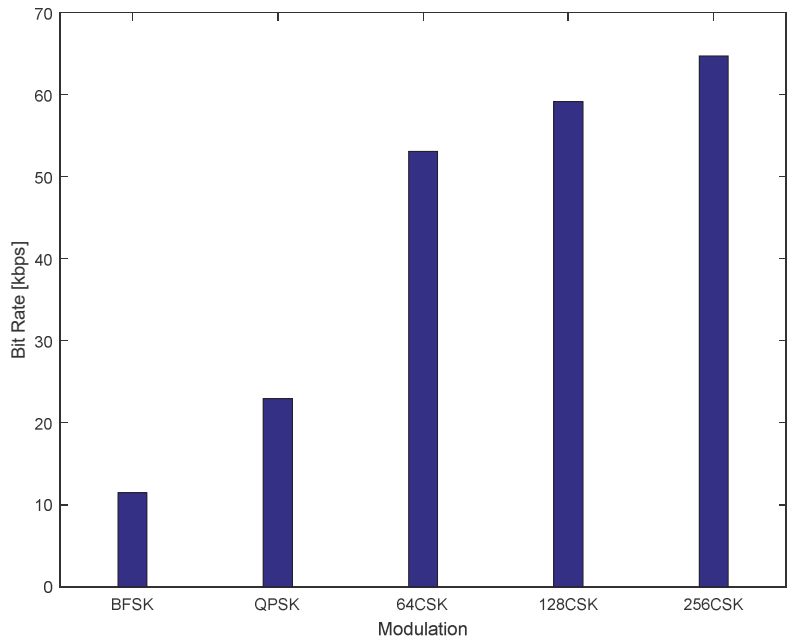

Figure 36. Maximum Bit Rates of Different Modulation Techniques

As shown in Figure 37, as we increase the probability of bit error from 10^{-6} to 10^{-2}, the maximum link bit rate increases. By allowing more errors, we can achieve a higher bit rate.

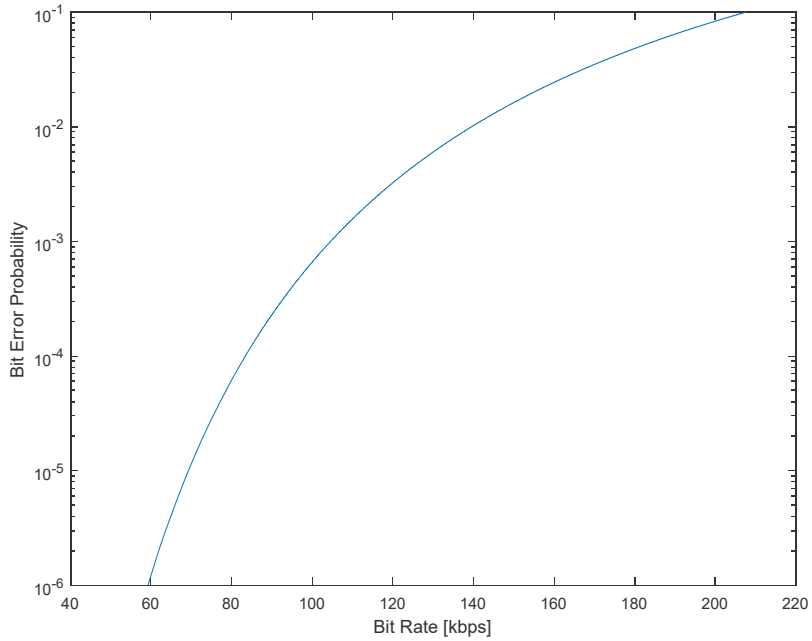

Figure 37. Maximum Bit Rate versus Bit Error Probability

3. Investigating the Link Margin for Uplink and Downlink

As the Cubesat is a regenerative satellite, both the uplink and downlink can use the same modulation technique. Since the inter-Cubesat propagation distance is 1340 km, which is almost three times longer than the propagation distance between the Cubesat and UAV, the inter-Cubesat links are considered the weakest links. In this case, both the uplink and downlink employ 128 CSK and support a bit rate of 56 kbps. A link budget analysis with both omni and directional antennas being used on a UAV are utilized in this example for the uplink and downlink paths. The calculations show that the usage of a directional antenna provides a 4.0 dB improvement in the link margin and a maximum uplink bit rate of 18.54 Mbps. Plots of the uplink and downlink margins and maximum bit rates are shown in Figure 38 and Figure 39, respectively.

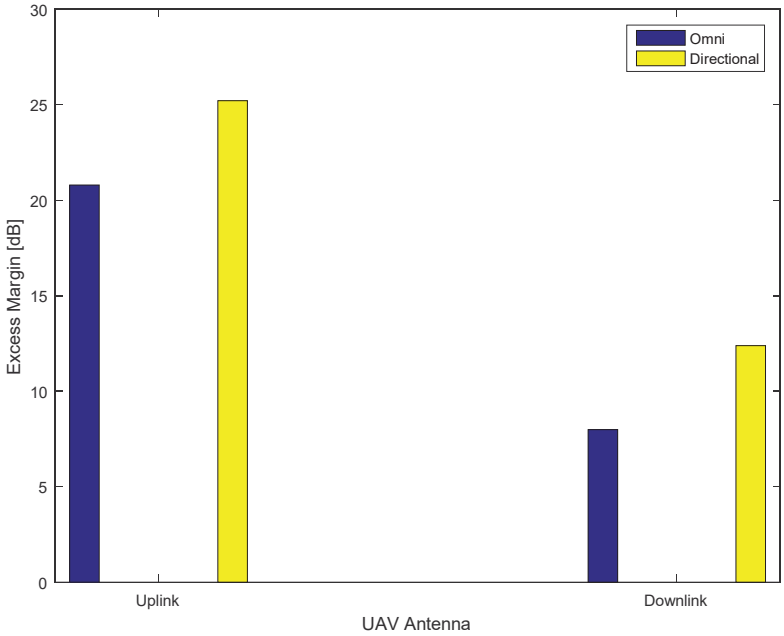

Figure 38. Link Margin for Uplink and Downlink

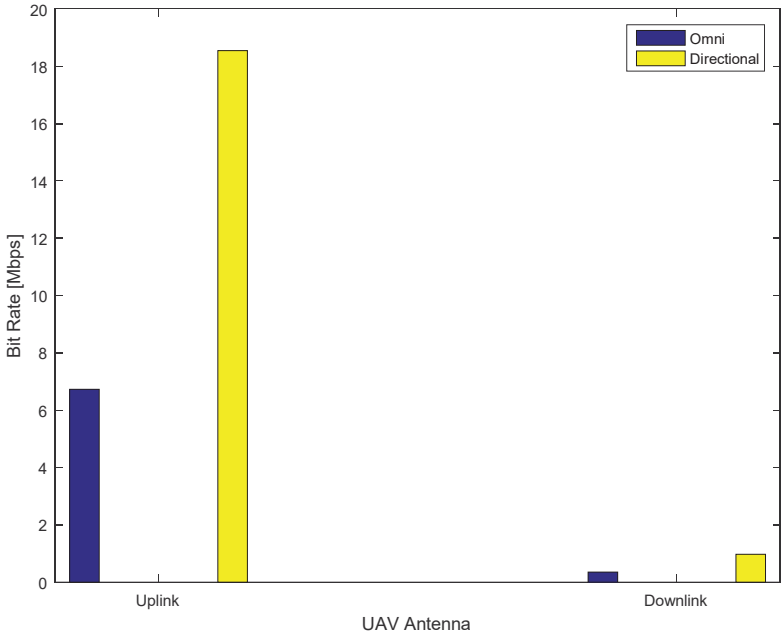

Figure 39. Maximum Bit Rate for Uplink and Downlink

E. PROPAGATION DELAY ANALYSIS

In this section, we analyze the propagation time delay of the proposed constellation using a few possible examples in intra-plane and inter-plane hop scenarios at different orbital heights. Intra-plane hop refers to the communication link between adjacent Cubesats within the same plane, while inter-plane hop refers to the communication link between Cubesats in adjacent planes. The four different scenarios analyzed for inter-plane hops are as follows:

- Inter-plane hop scenario 1: Cubesats moving in the same direction at the point of convergence
- Inter-plane hop scenario 2: Cubesats moving in the opposite directions from the point of convergence
- Inter-plane hop scenario 3: Cubesats moving along the divergence region
- Inter-plane hop scenario 4: Cubesat A on Plane 1 establishing a link with Cubesat B on Plane 2 in the divergence region

1. Intra-plane Hop

First, we begin the discussion of the intra-plane hop scenario. For simplicity, two Cubesats depicting the communication link to be analyzed are illustrated in Figure 40.

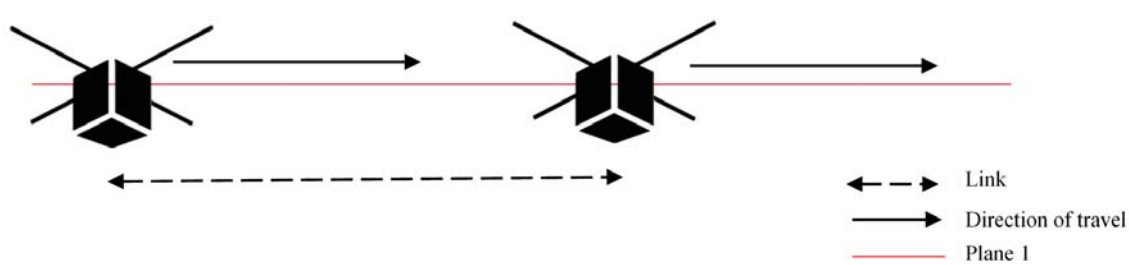

Figure 40. Intra-plane Hop

Based on the number of satellites per plane required at each proposed orbital height, we derive the intra-plane separation distance d_1 between two adjacent Cubesats using

$$d_1 = \left(r_e + h\right)\frac{2\pi}{n} \tag{16}$$

where n is the number of Cubesats per plane. As discussed earlier with regard to (13), the propagation time delay is directly related to the separation distance.

With the decrease in the orbital height, there is a need for more Cubesats per plane in order to achieve the desired performance coverage. An increase in the number of Cubesats per plane reduces the separation distance between the adjacent Cubesats. Correspondingly, this reduces the propagation time delay. The result of the propagation delay at different orbital heights is shown in Figure 41. The MATLAB simulation codes to obtain Figure 41 are shown in Appendix D.

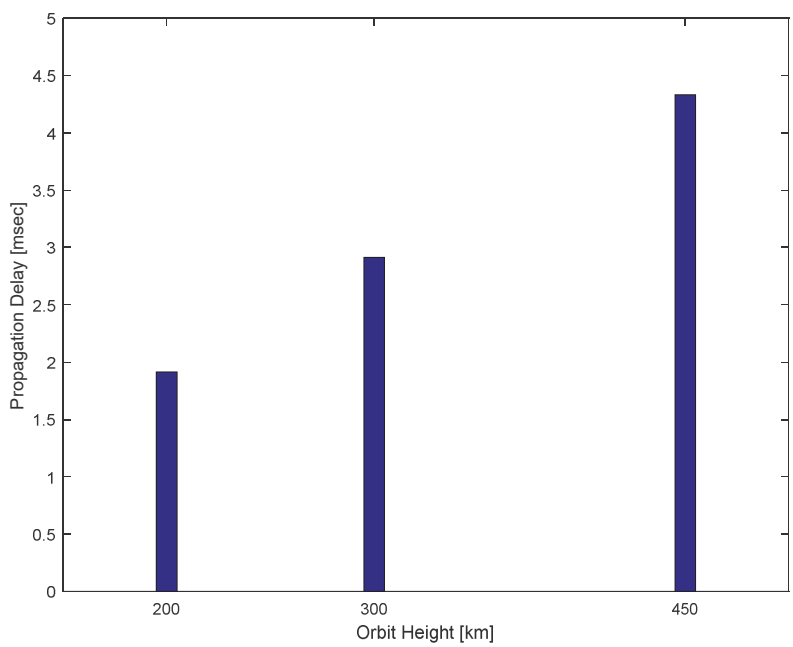

Figure 41. Propagation Time Delay for Different Orbit Heights

2. Inter-plane Hop

(1) Scenario 1—Cubesats Moving in the Same Direction at the Point of Convergence

With the Cubesats densely located at the convergence point, there is a shorter separation distance d_2, and the inter-plane separation distance is given by [51]

$$d_2 = (r_e + h)\frac{2\pi}{N} \tag{17}$$

where N is the total number of Cubesats in a constellation and $2\pi/N$ refers to the relative phasing parameter of Cubesats mentioned in [32]. A shorter d_2 leads to a decrease in the propagation time delay. The illustration for scenario 1 is shown in Figure 42.

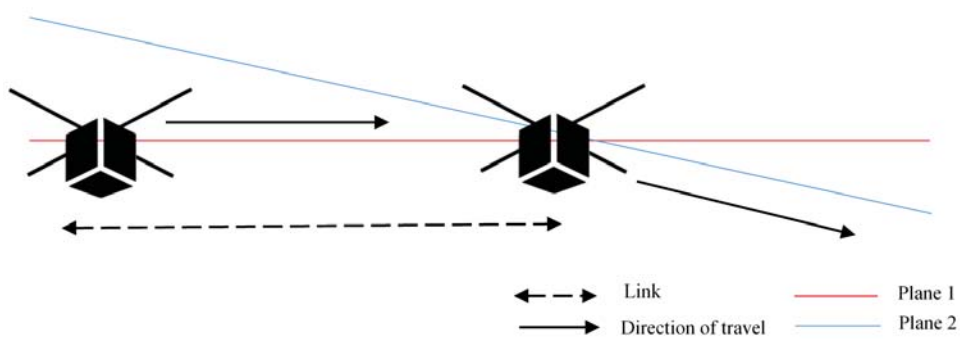

Figure 42. Inter-plane Hop Scenario 1

(2) Scenario 2—Cubesats Moving in the Opposite Directions from Point of Convergence

This scenario looks at the separation distance of the Cubesats when they are moving in opposite directions from the converging point, as shown in Figure 43. Based on geometry, the shortest separation distance occurs when both Cubesats are a distance $d_2/2$ from the converging point, and the shortest separation distance d_3 between two Cubesats is approximated as

$$d_3 = \frac{d_2}{2}\left(\frac{\pi}{P}\right) \tag{18}$$

where P is the number of orbital planes. The derivation of d_3 is shown in Appendix E. As d_3 is significantly smaller than d_2, the minimum propagation delay time between two Cubesats is illustrated in this scenario.

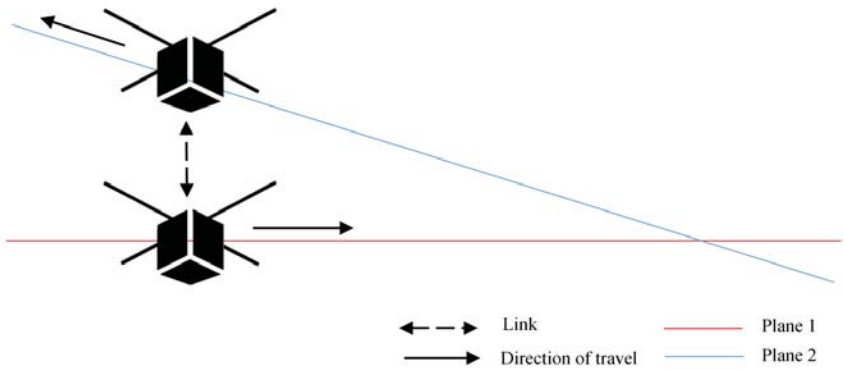

Figure 43. Inter-plane Hop Scenario 2

(3) Scenario 3—Cubesats Moving along the Divergence Region

As opposed to scenario 1, if the convergence point is at the equatorial region, the divergence point is at the polar region. As the Cubesats move along the plane in the divergence region, the separation distance d_4, which is dependent on the number of planes, is given by [51]

$$d_4 = \left(r_e + h\right)\frac{\pi}{P}. \tag{19}$$

This scenario is illustrated in Figure 44.

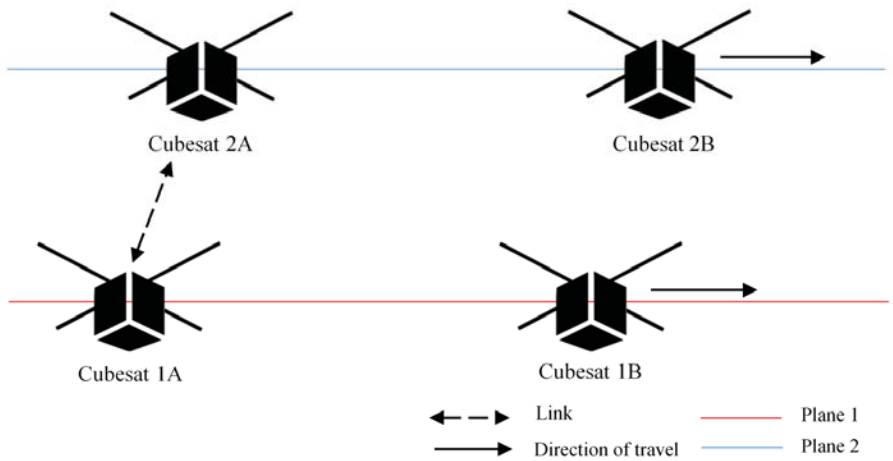

Figure 44. Inter-plane Hop Scenario 3

(4) Scenario 4—Cubesat A on Plane 1 Establishing a Link with Cubesat B on Plane 2 in the Divergence Region

Cubesats moving along different planes in the divergence region at the same orbital height are analyzed here. For this case, Cubesat 1A establishes a direct link with Cubesat 2B instead of the typical approach of double hopping from the Cubesats in the same plane followed by an inter-orbital plane hop to Cubesat 2B; i.e., hopping from Cubesat 1A to Cubesat 1B and then to Cubesat 2B.

As the inter-plane separation distance d_4 is similar to distance d_1, and knowing that the intra-plane separation distance is d_1, the separation distance between Cubesat 1A and Cubesat 2B is approximately $\sqrt{2}d_1$. This scenario is illustrated in Figure 45.

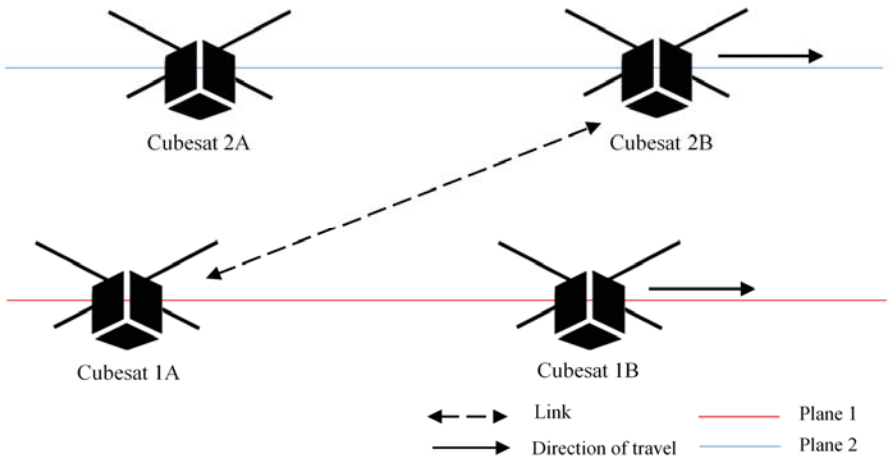

Figure 45. Inter-plane Hop Scenario 4

For these four scenarios, we evaluated the propagation time delay of the Cubesat links in the polar and inclined constellations; analysis at orbital heights of 200 km, 300 km and 450 km was performed. The propagation time delay was calculated based on the satellite separation distances listed in Tables 7 to 9. The results of the analyses are plotted in Figure 46 and Figure 47. The MATLAB simulation codes to obtain Figure 46 and Figure 47 are shown in Appendix D.

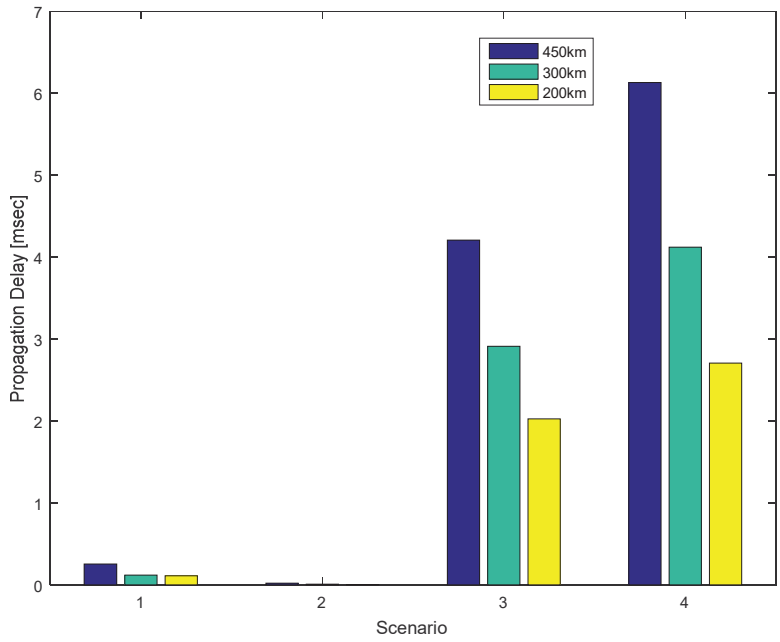

Figure 46. Propagation Time Delay of Inter-plane Hops with Polar Configuration

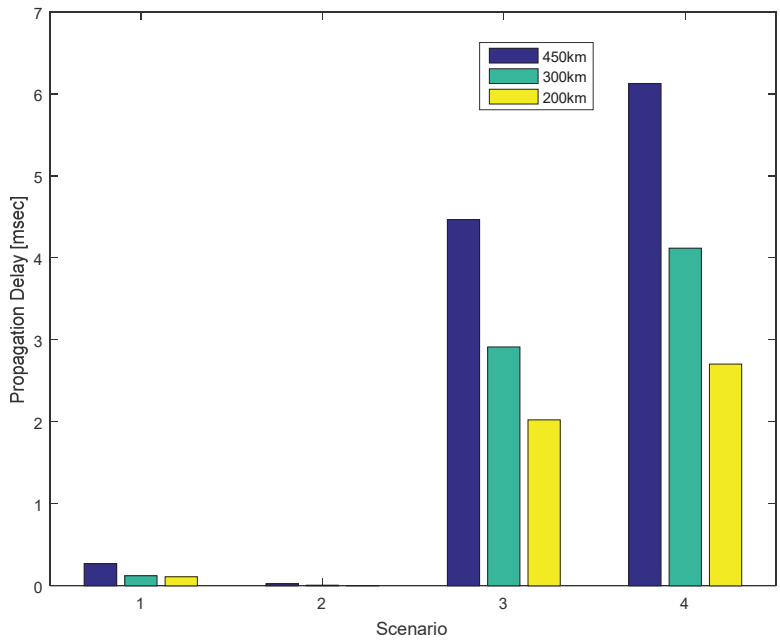

Figure 47. Propagation Time Delay of Inter-plane Hops with Inclined Configuration

We observe that the propagation time delay of one hop is proportional to the separation distance between two Cubesats. From Figure 46 and Figure 47, regardless of the constellations, we conclude that the minimum and maximum propagation time delays can be obtained from scenarios 2 and 4, respectively. At the selected orbital height of 450 km, the minimum propagation time delay is between 23.6 μs to 26.6 μs, while the maximum propagation time delay is 6.13 ms.

For scenario 4, although the time delay is reduced with the direct single hop configuration as opposed to the double hop, the bit rate is halved as the link margin has to be reduced by approximately 3.0 dB to compensate for the additional separation distance. Scenario 3 is the typical propagation time delay and is similar to the time delay of the intra-plane hop.

When comparing the propagation delay of a GEO satellite with that of a Cubesat at the orbital height of 450 km, we see the propagation time delay is reduced from 240 ms to 4.5 ms. The multi-hop connectivity of the Cubesats yields significant improvements to the time delay and is suitable for real-time communication links that require low latency. There could be a performance trade-off in a multiple hop configuration as each hop introduces more delays such as processing and queuing delays.

THIS PAGE INTENTIONALLY LEFT BLANK

V. CONCLUSIONS AND FUTURE WORK

In this thesis, theoretical studies were carried out to investigate the best constellation design to provide continuous global coverage and the highest supportable bit rate. One of the principle contributions of this work was the affirmation of the feasibility of using a Cubesat constellation as an alternative communication backbone to achieve continuous global coverage. From a suite of space parameters of orbital mechanics parameters, we identified the key elements required to determine the optimal height of our Cubesat constellation while meeting our mission requirement. These parameters are namely collision avoidance, Cubesat decay lifetime, and footprint.

Next, we proposed the use of polar and inclined constellations based on Walker's and modified SOC designs, respectively. Both the polar and inclined Cubesat constellation designs were generated for three different orbital heights. From there, we determined a methodology based on the optimal number of planes and total number of satellites needed in the Cubesat constellation; this methodology was verified using the STK stimulation program. Finally, we performed a link budget analysis and optimized the communication links to achieve a higher data rate while still fulfilling the mission requirements.

Following is a summary of the results:

- The Cubesat constellation at 450 km is recommended as it requires the least number of satellites and also has the longest decay lifespan. A Cubesat constellation of 17 planes with 33 satellites per plane is proposed for the polar constellation design while 16 planes with 33 satellites per plane is proposed for the inclined constellation design.
- With existing COTS hardware, the Cubesat is able to achieve a theoretical bit rate of 11.46 kbps at 450 km. This bit rate can be further improved through the employment of MCSK. With 128-CSK, the maximum theoretical bit rate is 59.2 kbps, which is a 7.0 dB improvement.
- With the ISL having the longest propagation distance, it is considered the weakest link as compared to the uplink channel from the UAV to Cubesat or downlink channel from Cubesat to UAV; thus, the capacity of the channel is limited to 59.2 kbps.

These results reinforced the idea that Cubesats are suitable selection as the communication backbone architecture with the ability to provide continuous global coverage for a network of UAVs or other communication nodes. The effectiveness of the architecture is more apparent if the operational profile is restricted to a region; i.e., the establishment of communication links that require the minimal number of hops.

We recommend areas for future research. First, the theoretical research work should be implemented in actual hardware. The Cubesats constellation can be built using COTS hardware to verify its performance with theoretical results. Cubesat transceivers that support 128-CSK modulation can be further explored and developed so that these transceivers can be incorporated into the hardware implementation. As a result, the performance of 128-CSK transceivers can be compared with that of BFSK transceivers currently available on the market.

Next, the STK simulation of the constellation can be further enhanced by integrating it with the EXata stimulation program by Scalable Network Technologies. EXata allows network simulations and evaluations of the ISL performance together with the communication nodes such as UAVs and ground stations. Network parameters in the physical, medium access control protocol, and routing protocols can be specified for various simulations. Networking protocols and network performance in terms of delay, throughput, and drop rate can be further studied and analyzed.

In addition, if there is an operational need to deploy Cubesats on a two-layer constellation design at the orbital height of 200 km, additional studies on collision avoidance and the communication aspect between adjacent planes of different heights needs to be investigated.

In conclusion, with increasing advances in technology, there is a high potential for the implementation of Cubesats utilizing optical communication links and the promise of significantly higher data rates in the near future.

APPENDIX A. STEPS TO SIMULATE THE DECAY LIFETIME OF CUBESAT IN STK.

1. Use “Insert STK Objects” window to insert a Cubesat.

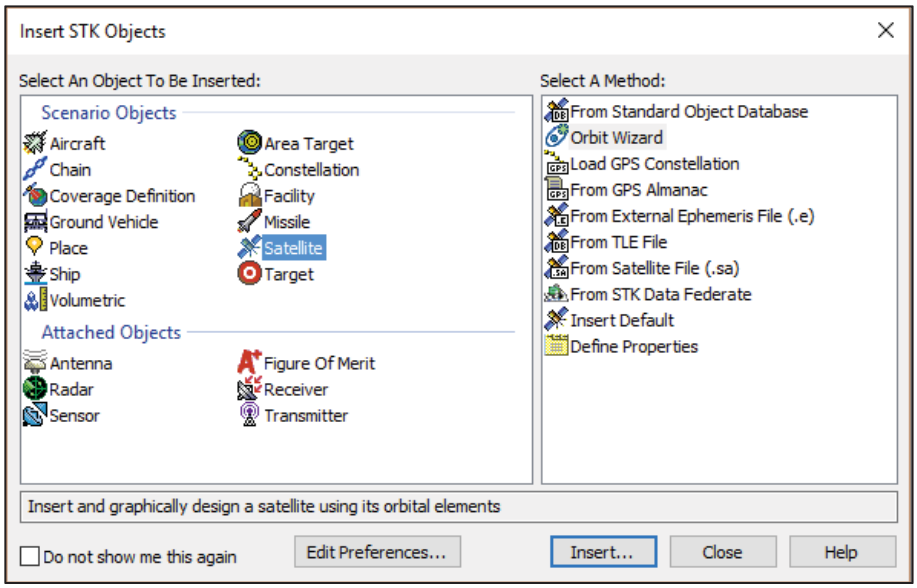

2. Configure the Cubesat parameters such as orbital height and inclination value using “Orbit Wizard.” Select “OK,” and a Cubesat is generated.

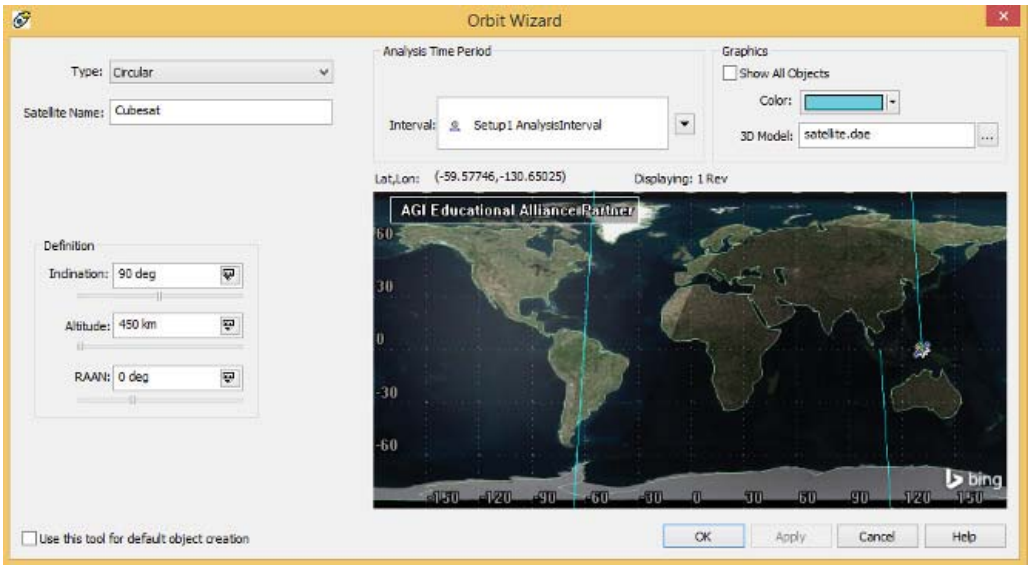

3. Go to "Object Browser," and select the newly created Cubesat. Select "Lifetime" under "Satellite."

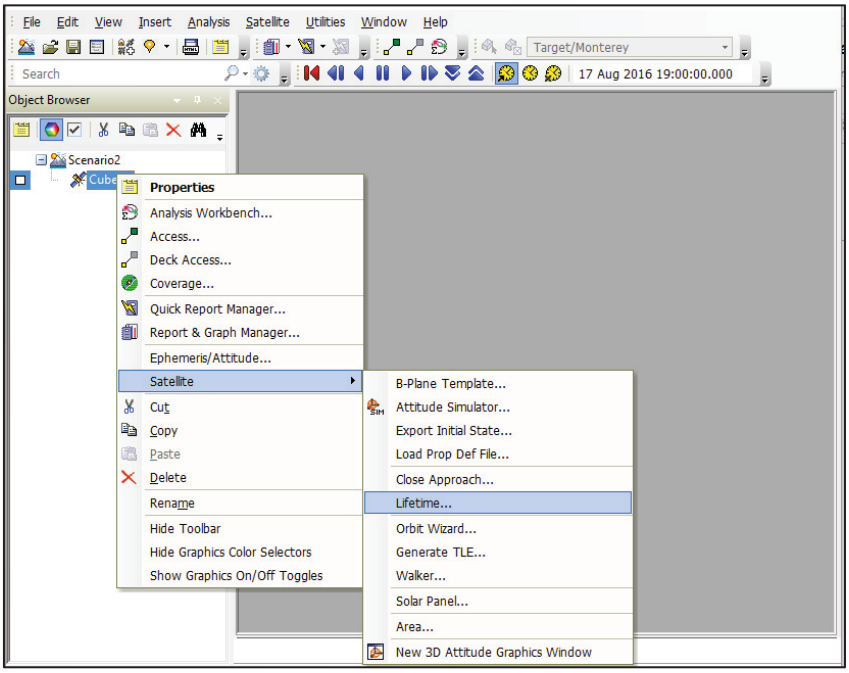

4. Define the "Satellite Characteristics" and "Solar Data." Jacchia 1971 is commonly used in the decay lifetime estimation to model atmospheric density. Select "Compute" to generate the decay lifetime result.

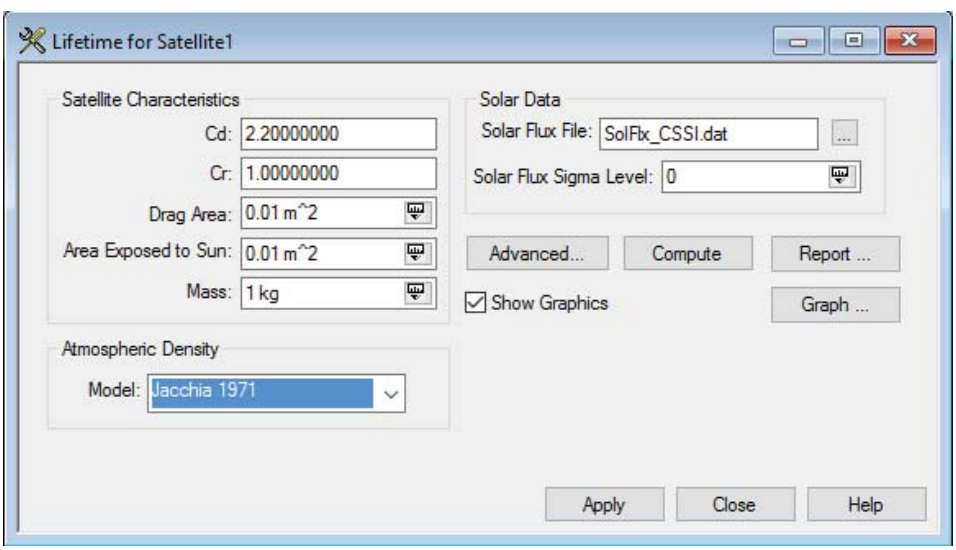

APPENDIX B. STEPS TO SIMULATE THE COVERAGE OF THE CUBESAT CONSTELLATION IN STK

1. Use "Insert STK Objects" window to insert a location using "From City Database."

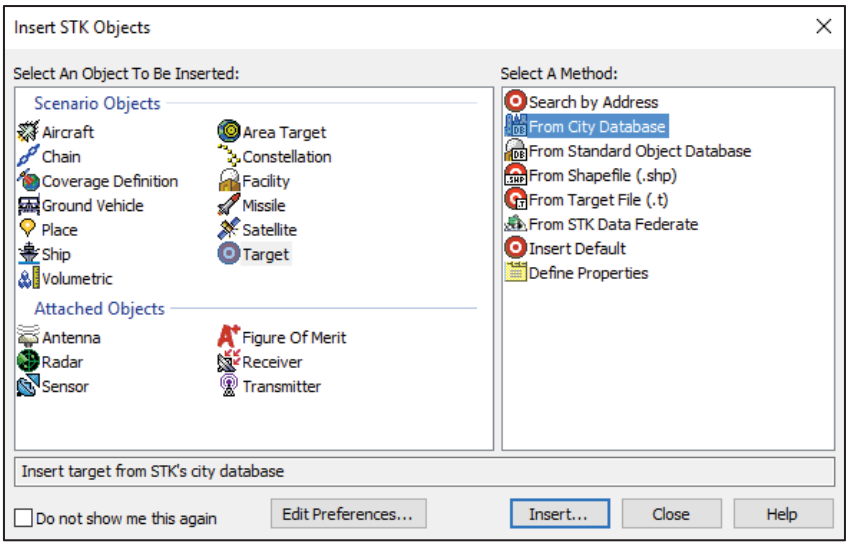

2. Type in the name of the city and select the corresponding city from the database.

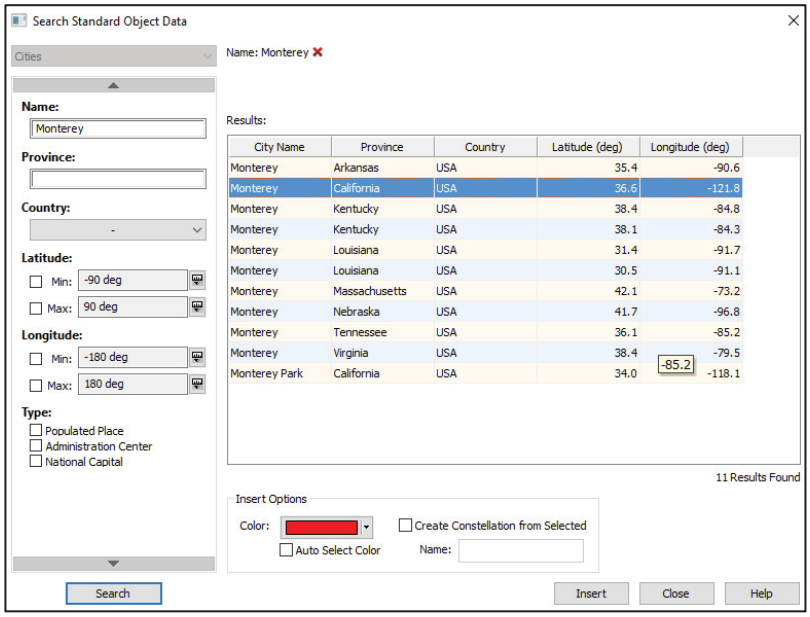

3. Use “Insert STK Objects” window to insert a Cubesat.

4. Configure the Cubesat parameters such as the orbital height and inclination value using “Orbit Wizard.” Select “OK” and a Cubesat is generated. This Cubesat is the seed satellite to create a Cubesat constellation.

5. Next, go to “Object browser” and select the newly created Cubesat. Select “Walker” as the satellite.

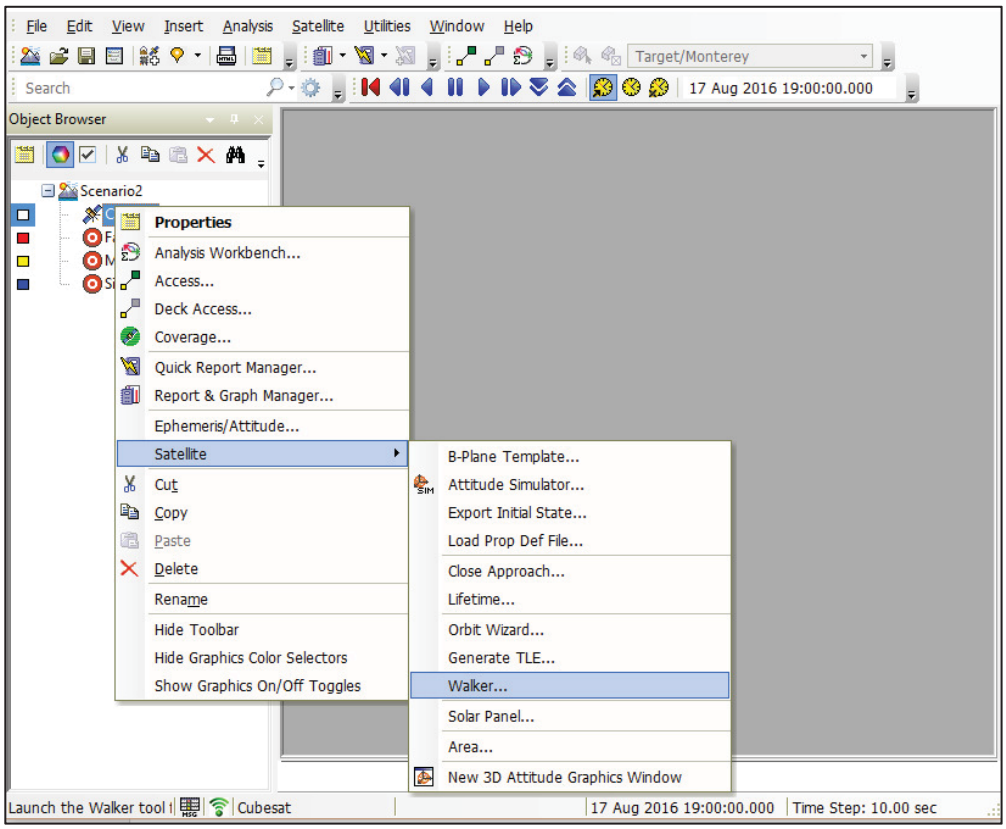

6. Use the “Walker Tool” to generate the required constellation. Configure the “Number of Planes” and “Number of Sats per Plane.” Select “Create Constellation” and create a name for the constellation.

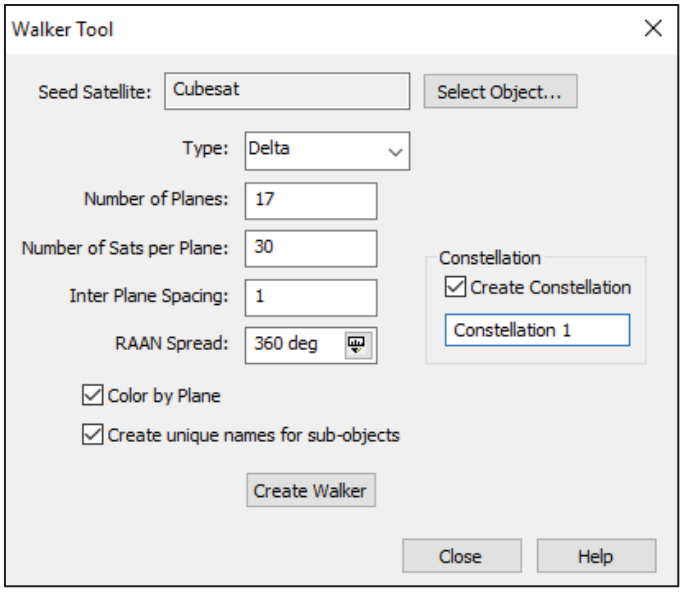

7. From the “Analysis” tab, select “Coverage.”

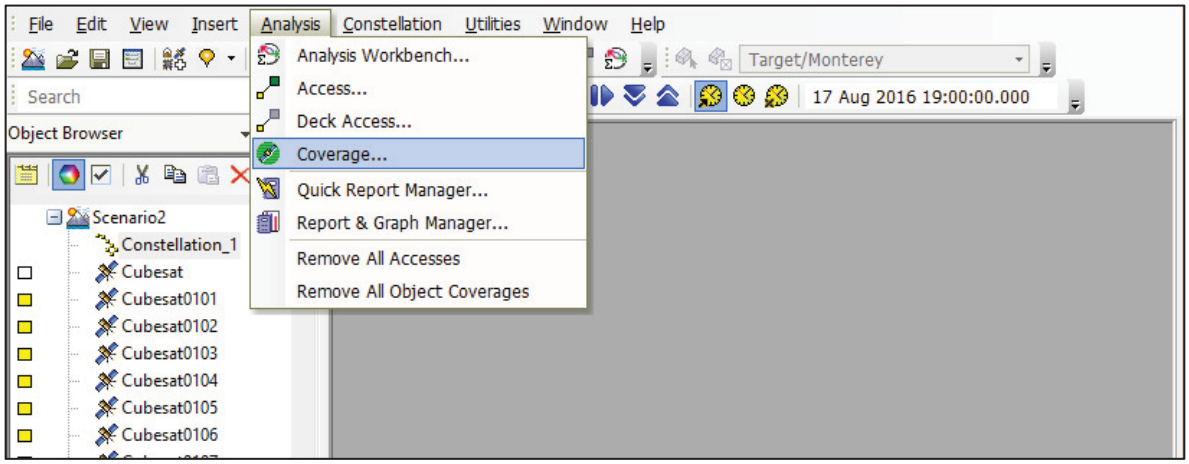

8. Click “Select Object” to choose the location for the simulation.

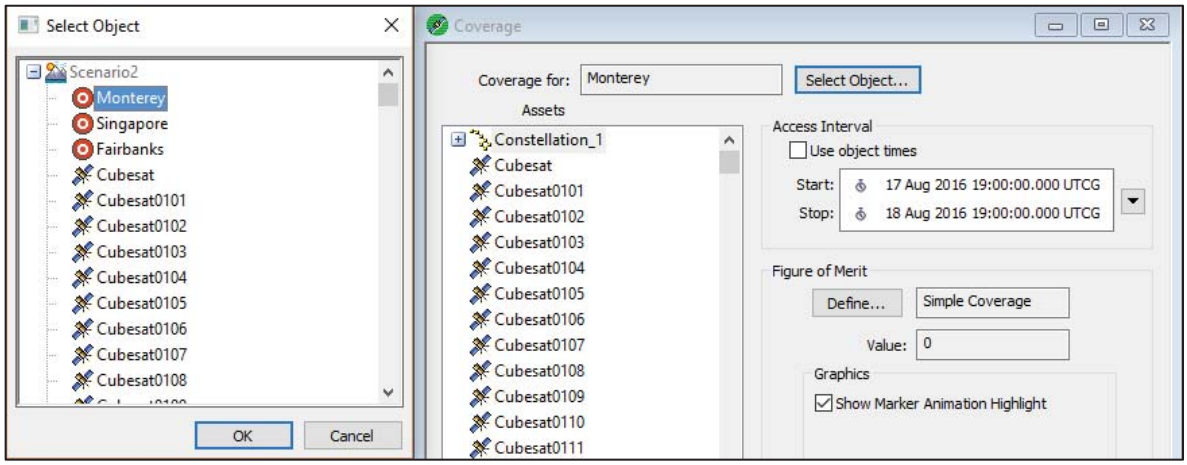

9. Select the pre-determined constellation, and select “Assign,” followed by “Compute” to generate the coverage for the selected location. Go to “Reports” to obtain the simulation results.

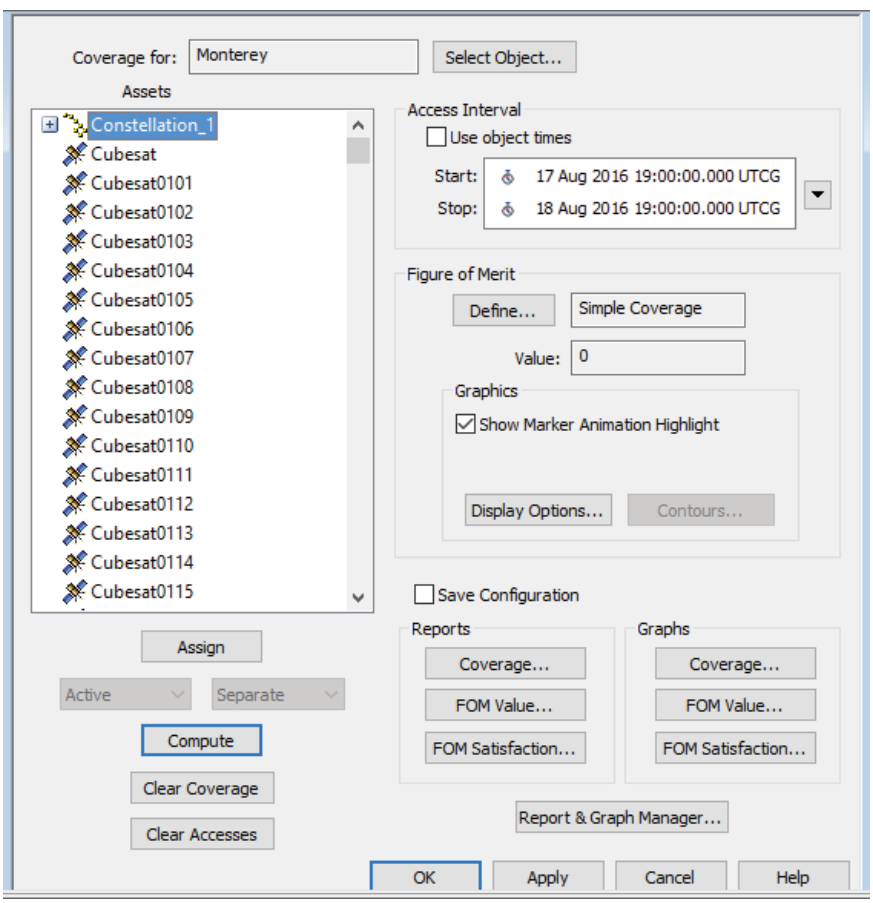

APPENDIX C. MATLAB CODES FOR LINK PERFORMANCE OPTIMIZATION

This part of the analysis refers to MATLAB codes used to derive the results from Figure 32 to Figure 39 in Chapter IV.

1. The MATLAB codes for generating Figure 32 and Figure 33 is as shown.

```
%Link budget analysis of Inter-Cubesat links @ 200km, 300km, 450km using BFSK

%Constant
c=3e8; %Speed of light
K=1.38e-23; %Boltzmann constant
Re=6378e3; %Radius of earth

%Parameter
freq=435e6; %Operating frequency
lamda=c/freq; %Wavelength
height= [200 300 450]; %Orbit height of Cubesat
M=4; %QPSK Modulation technique

%Transmitter parameter
Power=1; %Transmit power in watt
Pt=10*log10(Power); %Transmit power in dB
Gt=0.6; %Transmitter antenna gain in dB
Lt=1; %Other transmitter losses in dB such as insertion loss
EIRP=Pt+Gt-Lt; %Equivalent Isotropic Radiated Power

%Total propagation loss
d=[607.81 874.15 1340.67]; %Distance between two Cubesat in km
Lc= 20*log10(4*pi.*d*1000/lamda); %Free space propagation loss
Lp=3; % Polarization losses in dB (Circular polarization for both satellites)
La=0; %Other losses in dB
L=Lc+Lp+La, %Total losses in dB

% Receiver parameter
Gr0=0.6; %Receiver antenna gain in dB
Lr=1; %Other receiver losses in dB such as insertion loss
Gr=Gr0-Lr;%Total receiver gain in dB

%Received Power and Energy per Bit
Pr=EIRP-L+Gr, %Power Received in dB
```

```
BitRate=[9.6e3 9.6e3 9.6e3], %Bit rate
SymbolRate=BitRate/log2(M), %Symbol Rate
Rb= 10*log10(BitRate), %Bit rate in dB
Eb=Pr-Rb, %Energy per bit in dB

%Noise computation
Tsys=390; %Receiver System Temp in kelvin
No=10*log10(K*Tsys), %Receive noise power spectral in dB

%Link margin computation
EbNo=Eb-No, %Eb/No computed in dB
EbNo_req=13.54; %Eb/No required in dB to achieve bit error probability of 1e-6
Coding=6; %Coding gain in dB
Margin=3; %Margin required in dB
Excess_Margin=EbNo-EbNo_req+Coding-Margin, %Extra margin in dB

%Minimum Transmitted Power
NewPt=Pt-Excess_Margin;
NewPower=10.^[NewPt/10],

figure
name= {'200';'300';'450'};
x = [1:3];
bar(x,NewPower, 0.2)
set(gca,'xticklabel',name)
xlabel ('Height [km]')
ylabel ('Transmit Power [W]')

% Maximum Bit Rate
figure
NewRb=Rb+Excess_Margin;
NewBitrate=10.^[NewRb/10],
bar(x,NewBitrate/1000, 0.2)
set(gca,'xticklabel',name)
xlabel ('Height [km]')
ylabel ('Bit Rate [kbps]')
```

2. The MATLAB codes for generating Figure 34, Figure 35 and Figure 36 is as shown.

```
%Link budget analysis of Inter-Cubesat links @ 450km using
%BFSK QPSK, 64CSK, 128CSK, 256CSK

%Constant
c=3e8; %Speed of light
K=1.38e-23; %Boltzmann constant
Re=6378e3; %Radius of earth

%Parameter
freq=435e6; %Operating frequency in Hz
lamda=c/freq; %Wavelength
height=450; %Orbit height of Cubesat in km
M=[2 4 64 128 256]; %M-ary Modulation

%Transmitter parameter
Power=1; %Transmit power in watt
Pt=10*log10(Power); %Transmit power in dB
Gt=0.6; %Transmitter antenna gain in dB
Lt=1; %Other transmitter losses in dB such as insertion loss
EIRP=Pt+Gt-Lt; %Equivalent Isotropic Radiated Power

%Total propagation loss
d=[1340.67 1340.67 1340.67 1340.67 1340.67]; %Distance between two Cubesat in
km
Lc= 20*log10(4*pi.*d*1000/lamda); %Free space propagation loss
Lp=3; % Polarization losses in dB (Circular polarization for both satellites)
La=0; %Other losses in dB
L=Lc+Lp+La, %Total losses in dB

% Receiver parameter
Gr0=0.6; %Receiver antenna gain in dB
Lr=1; %Other receiver losses in dB such as insertion loss
Gr=Gr0-Lr;%Total receiver gain in dB

%Received Power and Energy per Bit
Pr=EIRP-L+Gr, %Power Received in dB
BitRate=[9.6e3 9.6e3 9.6e3 9.6e3 9.6e3], %Bit rate
SymbolRate=BitRate./log2(M), %Symbol Rate
Rb= 10*log10(BitRate), %Bit rate in dB
Eb=Pr-Rb, %Energy per bit in dB

%Noise computation
```

```
Tsys=390; %Receiver System Temp in kelvin
No=10*log10(K*Tsys), %Receive noise power spectral in dB

%Link margin computation
EbNo=Eb-No, %Eb/No computed in dB
EbNo_req=[13.54 10.53 6.88 6.41 6.02]; %Eb/No required in dB to achieve bit error
probability of 1e-6
Coding=6; %Coding gain in dB
Margin=3; %Margin required in dB
Excess_Margin=EbNo-EbNo_req+Coding-Margin, %Excess margin in dB

figure
modulation= {'BFSK';'QPSK';'64CSK';'128CSK';'256CSK'};
x = [1:5];
bar(x,Excess_Margin, 0.2)
set(gca,'xticklabel',modulation)
xlabel ('Modulation')
ylabel ('Excess Margin [dB]')

%Minimum Transmit Power
figure
NewPt=Pt-Excess_Margin;
NewPower=10.^[NewPt/10],
bar(x,NewPower, 0.2)
set(gca,'xticklabel',modulation)
xlabel ('Modulation')
ylabel ('Transmit Power [W]')

% Maximum Bit Rate
figure
NewRb=Rb+Excess_Margin;
NewBitrate=10.^[NewRb/10],
bar(x,NewBitrate/1000, 0.2)
set(gca,'xticklabel',modulation)
xlabel ('Modulation')
ylabel ('Bit Rate [kbps]')
```

3. The MATLAB codes for generating Figure 37 is as shown.

```
%Link budget analysis of Inter-Cubesat links @ 450km using 128CSK

%Constant
c=3e8; %Speed of light
K=1.38e-23; %Boltzmann constant
Re=6378e3; %Radius of earth

%Parameter
freq=435e6; %Operating frequency in Hz
lamda=c/freq; %Wavelength
height=450; %Orbit height of Cubesat in km
M=[128]; %M-ary Modulation

%Transmitter parameter
Power=1; %Transmit power in watt
Pt=10*log10(Power); %Transmit power in dB
Gt=0.6; %Transmitter antenna gain in dB
Lt=1; %Other transmitter losses in dB such as insertion loss
EIRP=Pt+Gt-Lt; %Equivalent Isotropic Radiated Power

%Total propagation loss
d=[1340.67]; %Distance between two Cubesat in km
Lc= 20*log10(4*pi.*d*1000/lamda); %Free space propagation loss
Lp=3; % Polarization losses in dB (Circular polarization for both satellites)
La=0; %Other losses in dB
L=Lc+Lp+La, %Total losses in dB

% Receiver parameter
Gr0=0.6; %Receiver antenna gain in dB
Lr=1; %Other receiver losses in dB such as insertion loss
Gr=Gr0-Lr;%Total receiver gain in dB

%Received Power and Energy per Bit
Pr=EIRP-L+Gr, %Power Received in dB

BitRate=[9.6e3], %Bit rate
SymbolRate=BitRate./log2(M), %Symbol Rate
Rb= 10*log10(BitRate), %Bit rate in dB
Eb=Pr-Rb, %Energy per bit in dB

%Noise computation
Tsys=390; %Receiver System Temp in kelvin
No=10*log10(K*Tsys), %Receive noise power spectral in dB
```

```
% To compute the Eb/No required to meet the bit error probability
Pb = [1e-6:1e-6:1e-1]; % Probability of bit error

% CSK Demodulator
M = [128],

% Upper bound of Coherent demodulator, Pb=(M/2)*qfunc(sqrt((Eb/No)*log2(M)))
EbNo_CoherentCSK=10*log10(((qfuncinv(2.*Pb/M)).^2)./(log2(M))),

%Link margin computation
EbNo=Eb-No, %Eb/No computed in dB
EbNo_req=EbNo_CoherentCSK; %Eb/No required in dB to achieve bit error
probability of 1e-6
Coding=6; %Coding gain in dB
Margin=3; %Margin required in dB
Excess_Margin=EbNo-EbNo_req+Coding-Margin, %Extra margin in dB

%Maximum Bit Rate
figure
NewRb=Rb+Excess_Margin;
NewBitrate=10.^[NewRb/10];

semilogy(NewBitrate/1000,Pb);
xlabel ('Bit Rate [kbps]')
ylabel ('Bit Error Probability')
```

4. The MATLAB codes for generating Figure 38 and Figure 39 are as shown.

```
%Link budget analysis of uplink from UAV to Cubesat @ 450km using 128CSK
%with omni and directional antenna.

%Constant
c=3e8; %Speed of light
K=1.38e-23; %Boltzmann constant
Re=6378e3; %Radius of earth

%Parameter
freq=440e6; %Operating frequency in Hz
lamda=c/freq; %Wavelength
height=450; %Orbit height of Cubesat in km
M=[128 128]; %M-ary Modulation

%Transmitter parameter
Power=6; %Transmit power in watt
Pt=10*log10(Power); %Transmit power in dB
```

```
Gt=[0.6 5]; %Transmitter antenna gain in dB
Lt=1; %Other transmitter losses in dB
EIRP=Pt+Gt-Lt; %Equivalent Isotropic Radiated Power

%Total propagation loss
d=[449 449]; %Distance between two Cubesat in km
Lc= 20*log10(4*pi.*d*1000/lamda); %Free space propagation loss
Lp=3; % Polarization losses in dB (Circular polarization for both satellites)
La=1.74; %Other losses in dB
L=Lc+Lp+La, %Total losses in dB

% Receiver parameter
Gr0=0.6; %Receiver antenna gain in dB
Lr=1; %Other receiver losses in dB
Gr=Gr0-Lr;%Total receiver gain in dB

%Received Power and Energy per Bit
Pr=EIRP-L+Gr, %Power Received in dB
BitRate=[56e3 56e3], %Bit rate
SymbolRate=BitRate./log2(M), %Symbol Rate
Rb= 10*log10(BitRate), %Bit rate in dB
Eb=Pr-Rb, %Energy per bit in dB

%Noise computation
Tsys=120; %Receiver System Temp in kelvin
No=10*log10(K*Tsys), %Receive noise power spectral in dB

%Link margin computation
EbNo=Eb-No, %Eb/No computed in dB
EbNo_req=[6.41 6.41]; %Eb/No required in dB to achieve bit error probability of 1e-
6
Coding=6; %Coding gain in dB
Margin=3; %Margin required in dB
Excess_Margin=EbNo-EbNo_req+Coding-Margin, %Excess margin in dB

%Link budget analysis of downlink from Cubesat @ 450km to UAV using 128CSK
%with omni and directional antenna.

%Constant
c=3e8; %Speed of light
K=1.38e-23; %Boltzmann constant
Re=6378e3; %Radius of earth

%Parameter
freq=430e6; %Operating frequency in Hz
```

```
lamda=c/freq; %Wavelength
height=450; %Orbit height of Cubesat in km
M=[128 128]; %M-ary Modulation

%Transmitter parameter
Power=1; %Transmit power in watt
Pt=10*log10(Power); %Transmit power in dB
Gt=[0.6 0.6]; %Transmitter antenna gain in dB
Lt=1; %Other transmitter losses in dB
EIRP=Pt+Gt-Lt; %Equivalent Isotropic Radiated Power

%Total propagation loss
d=[449 449]; %Distance between two Cubesat in km
Lc= 20*log10(4*pi.*d*1000/lamda); %Free space propagation loss
Lp=3; % Polarization losses in dB (Circular polarization for both satellites)
La=1.74; %Other losses in dB
L=Lc+Lp+La, %Total losses in dB

% Receiver parameter
Gr0=[0.6 5]; %Receiver antenna gain in dB
Lr=1; %Other receiver losses in dB
Gr=Gr0-Lr;%Total receiver gain in dB

%Received Power and Energy per Bit
Pr=EIRP-L+Gr, %Power Received in dB
BitRate=[56e3 56e3], %Bit rate
SymbolRate=BitRate./log2(M), %Symbol Rate
Rb= 10*log10(BitRate), %Bit rate in dB
Eb=Pr-Rb, %Energy per bit in dB

%Noise computation
Tsys=400; %Receiver System Temp in kelvin
No=10*log10(K*Tsys), %Receive noise power spectral in dB

%Link margin computation
EbNo=Eb-No, %Eb/No computed in dB
EbNo_req=[6.41 6.41]; %Eb/No required in dB to achieve bit error probability of 1e-
6
Coding=6; %Coding gain in dB
Margin=3; %Margin required in dB
Extra_Margin=EbNo-EbNo_req+Coding-Margin, %Extra margin in dB


figure
name= {'Uplink';'Downlink'};
```

```
x = [1:2];
Excess_Margin =[20.8, 25.2; 7.99, 12.39];
bar(x,Excess_Margin, 0.2)
set(gca,'xticklabel',name)
xlabel ('UAV Antenna')
ylabel ('Excess Margin [dB]')
legend ('Omni','Directional')

% Maximum Bit Rate
Rb=10*log10(56000);
NewRb=Rb+Excess_Margin;
NewBitrate=10.^[NewRb/10];

figure
bar(x,NewBitrate/1e6, 0.2)
set(gca,'xticklabel',name)
xlabel ('UAV Antenna')
ylabel ('Bit Rate [Mbps]')
legend ('Omni','Directional')
```

THIS PAGE INTENTIONALLY LEFT BLANK

APPENDIX D. MATLAB SIMULATION CODE FOR PROPAGATION DELAY ANALYSIS

MATLAB simulation was used to perform the propagation delay analysis for intra-plane and inter-plane hop scenarios.

1. The MATLAB codes for generation of Figure 41, Figure 46 and Figure 47 are shown.

```
%Propagation delay of the proposed constellation
c=3e8; %Speed of light
Re= 6378; %Earth Radius in km
H =[200 300 450]; %Orbital height of the Cubesat in km
SatNo= [72 48 33]; %Number of Sats per plane

Polar_PlaneNo= [34 24 17]; %Number of planes for polar
Inclined_PlaneNo= [34 24 16]; %Number of planes for inclined
Total_polar_SatNo= Polar_PlaneNo.*SatNo; %Total number of Sats for polar
Total_inclined_SatNo= Inclined_PlaneNo.*SatNo; %Total number of Sats for
inclined

%Intra Orbit Hop
Intra_A=2*pi./SatNo; %Angular seperation in rad
Intra_D=(Re+H).*Intra_A; %Dist seperation in km
Intra_delay=(Intra_D*1000/c*1000), %Propagation delay in msec

%Inter Orbit Hop
%Polar Configuration
Inter_polar_AP=pi./Polar_PlaneNo;%Angular seperation between plane in rad
Inter_polar_DP=(Re+H).*Inter_polar_AP; %Dist seperation between plane in km

Inter_polar_A=2*pi./Total_polar_SatNo.*[2 1 1]; %Angular seperation between
SATS in rad
Inter_polar_D=(Re+H).*Inter_polar_A; %Dist seperation between SATS in km

% Scenario 1: Cubesats moving in same direction at convergent point
Inter_polar_delay_1=(Inter_polar_D*1000/c*1000); %Propagation delay in msec

% Scenario 2:Cubesats moving in opposite direction at convergent point
Inter_polar_delay_2=0.5*(Inter_polar_D*1000/c*1000).*(pi./H); %Propagation
delay in msec

% Scenario 3: Cubesats moving in at most divergent point
Inter_polar_delay_3=(Inter_polar_DP*1000/c*1000); %Propagation delay in msec
```

```
% Scenario 4: Cubesats moving in at most divergent point
Inter_polar_delay_4=(sqrt(Inter_polar_DP.^2+Intra_D.^2)*1000/c*1000);
%Propagation delay in msec

%Inclined Configuration
Inter_inclined_AP=pi./Inclined_PlaneNo;%Angular seperation between plane in rad
Inter_inclined_DP=(Re+H).*Inter_inclined_AP; %Dist seperation between plane in
km

Inter_inclined_A=2*pi./Total_inclined_SatNo.*[2 1 1]; %Angular seperation
between SATS in rad
Inter_inclined_D=(Re+H).*Inter_inclined_A; %Dist seperation between SATS in km

% Scenario 1: Cubesats moving in same direction at convergent point
Inter_inclined_delay_1=(Inter_inclined_D*1000/c*1000); %Propagation delay in
msec

% Scenario 2:Cubesats moving in opposite direction at convergent point
Inter_inclined_delay_2=Inter_inclined_delay_1./2; %Propagation delay in msec

% Scenario 3: Cubesats moving in at most divergent point
Inter_inclined_delay_3=(Inter_inclined_DP*1000/c*1000); %Propagation delay in
msec

% Scenario 4: Cubesats moving in at most divergent point
Inter_inclined_delay_4=(sqrt(Inter_inclined_DP.^2+Intra_D.^2)*1000/c*1000);
%Propagation delay in msec

%Plot figure
bar(H,Intra_delay,0.1);
xlabel ('Orbit Height [km]');
ylabel ('Propagation Delay [msec]');
axis ([150 500 0 5]);

% Propagation Time Delay for Constellation with Polar Configuration
figure
A1=[Inter_polar_delay_1;Inter_polar_delay_2;Inter_polar_delay_3;Inter_polar_delay
_4];
bar(A1);

legend ('200km','300km','450km');
xlabel ('Scenario');
ylabel ('Propagation Delay [msec]');
```

```
% Propagation Time Delay for Constellation with Inclined Configuration
figure
A2=[Inter_inclined_delay_1;Inter_inclined_delay_2;Inter_inclined_delay_3;Inter_inc
lined_delay_4],
bar(A2);

legend ('200km','300km','450km');
xlabel ('Scenario');
ylabel ('Propagation Delay [msec]');
```

THIS PAGE INTENTIONALLY LEFT BLANK

APPENDIX E. MINIMUM CUBESAT SEPARATION DISTANCE FOR SCENARIO 2

This part of the analysis refers to the derivation of the minimum separation distance for Cubesats moving in opposite directions from the point of convergence.

1. At time zero, both Cubesats are separated by d_2.

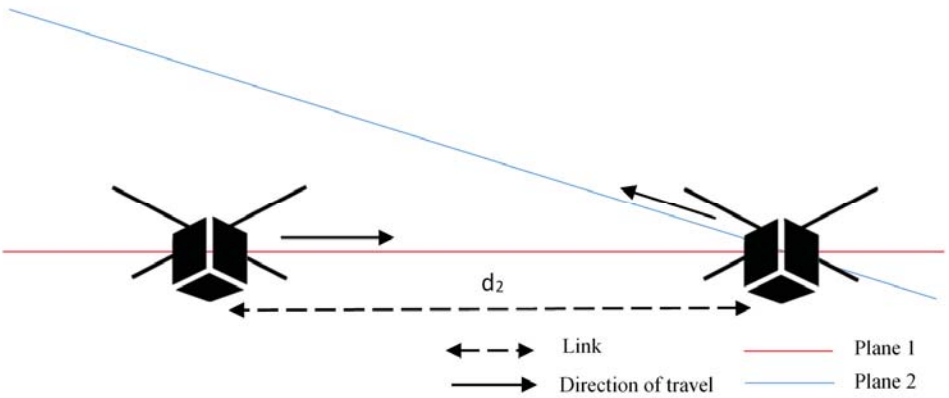

2. At time t', both Cubesats are still separated by d_2 as the Cubesats have moved in opposite directions from the converging point.

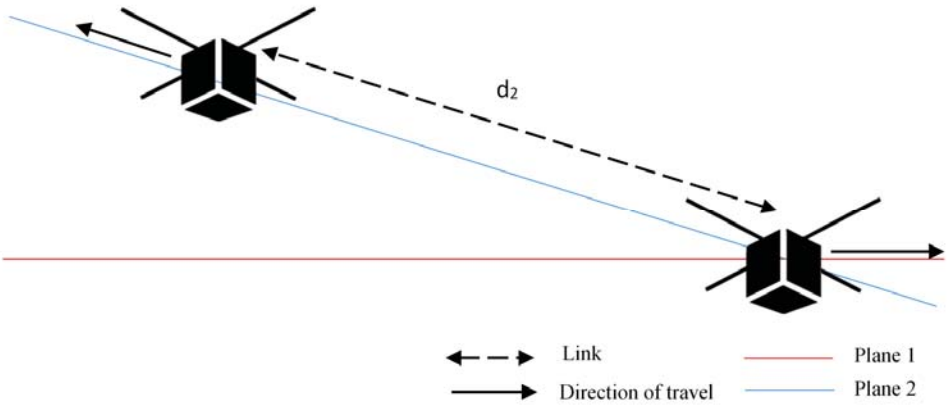

3. At time $t'/2$, both Cubesats are at $d_2/2$ from the converging point, and the separation distance between both Cubesats is the shortest. The shortest separation distance between two Cubesats can be derived using the small angle formula

$$d_3 = \frac{d_2}{2}\sin(\phi) = \frac{d_2}{2}(\phi) \tag{20}$$

where ϕ is the angular separation between adjacent planes.

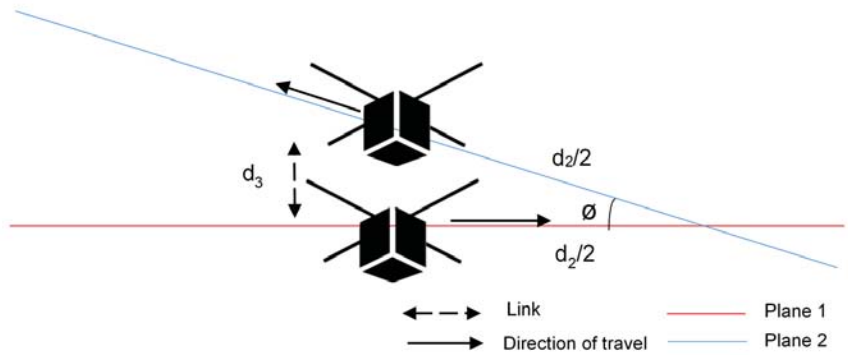

4. The minimum separation distance for a Cubesat constellation design of 17 planes with 33 satellites per plane at the orbital height of 450 km is given by [51]

$$d_2 = (r_e + h)\frac{2\pi}{(n \times p)} \tag{21}$$

$$= (6378 + 450)\frac{2\pi}{(33 \times 17)}$$

$$= 76.47\text{km}$$

and

$$d_3 = \frac{d_2}{2}(\phi) \tag{22}$$

$$= \frac{76.47}{2}\left(\frac{\pi}{17}\right)$$

$$= 7.07\text{km}$$

Though the minimum separation distance computed is less than the recommended separation distance of 25 km (typical distance for large LEO satellites), the probability of collision is remote and still acceptable. This is because the Cubesat size relative to the separation distance is significantly smaller, and only one pair of orbital planes in a constellation exhibits movement in opposite directions.

THIS PAGE INTENTIONALLY LEFT BLANK

LIST OF REFERENCES

[1] S. Cakaj, B. Kamo, A. Lala, and A. Rakipi, "The coverage analysis for low earth orbiting satellites at low elevation," in *Int. J. Adv. Comput. Sci. App.*, 2014, vol. 5, no. 6, Available: http://dx.doi.org/10.14569/IJACSA.2014.050602.

[2] A. Babuscia, B. Corbin, R. Jensen-Clem, M. Knapp, I. Sergeev, M. Van de Loo, and S. Seager, "Commcube 1 and 2: A Cubesat series of missions to enhance communication capabilities for CubeSat," in *Proceedings of IEEE Aerospace Conference,* 2013, pp. 1–19.

[3] A. D. Santangelo and P. Skentzos, "Utilizing the Globalstar network for satellite communications in low earth orbit," present in 54th AIAA Aerospace Sciences Meeting, San Diego, CA, 2016.

[4] A. Budianu, T. J. W. Castro, A. Meijerink, and M. J. Bentum, "Inter-satellite links for Cubesats," in *Proceedings of IEEE Aerospace Conference*, 2013, pp. 1–10.

[5] H. Bedon, C. Negron, J. Llantoy, C. M. Nieto, and C. O. Asma, "Preliminary internetworking simulation of the qb50 Cubesat constellation," in *Proceedings of IEEE Latin-American Conference on Communications*, 2010, pp. 1–6.

[6] B. Yanar, "Dynamic extension of network for cyber and communication." M.S. thesis, Dept. ECE, Naval Postgraduate School, Monterey, CA, 2016.

[7] A. Ellis, M. Mercury, and S. Brown, "Global coverage from ad-hoc constellations in rideshare orbits," presented at 26th AIAA/USU Small Satellite Conference, Logan, UT, 2012.

[8] A. Marinan, A. Nicholas, and K. Cahoy, "Ad hoc Cubesat constellations: secondary launch coverage and distribution," in *Proceedings of IEEE Aerospace Conference*, 2013, pp. 1–15.

[9] T. Guillemin. (n.d.). LEO and GEO Constellations: 7 elements to consider before joining the debate. [Online]. Available: http://www.intelsat.com/newsletter/IntelsatInsider/2nd_Quarter_2015/Article_1.html. Accessed Jul, 15, 2016.

[10] M. Swartwout, "The first one hundred cubesats: A statistical look," *Journal of Small Satellites,* vol. 2, pp. 213–233, 2013.

[11] Saint Louis University CubeSat Database. [Online]. Available: https://sites.google.com/a/slu.edu/swartwout/home/cubesat-database. Accessed Jun. 30, 2016.

[12] A. J. Vazquez-Alvarez, R. Tubio-Pardavila, A. Gonzalez-Muino, F. Aguado-Agelet, M. Arias-Acuna, and J. A. Vilan-Vilan, "Design of a polarization diversity system for ground stations of Cubesat space systems," *IEEE Antennas and Wireless Propagation Letters*, 2012, vol. 11, pp. 917–920.

[13] S. Ramsey. (2015, Oct. 14). NASA awards venture class launch services contracts for cubesat satellites. [Online]. Available: http://www.nasa.gov/press-release/nasa-awards-venture-class-launch-services-contracts-for-cubesat-satellites

[14] C. Clark, A. Chin, P. Karuza, D. Rumsey, and D. Hinkley, "CubeSat communications transceiver for increased data throughput," in *Proceedings of IEEE Aerospace Conference*, 2009, pp.1–5.

[15] Hiscock Radiation Belt Explorer. (n.d.). Montana State University. [Online]. Available: https://ssel.montana.edu/e1p.html. Accessed Jul. 15, 2016.

[16] P. Keane. (2013, May. 24). How to de-orbit a cubesat. *Space safety* [Online]. Available: http://www.spacesafetymagazine.com/space-debris/debris-removal/de-orbit-cubesat/

[17] A. Addaim, A. Kherras, and E. B. Zantou, *Design of Low-Cost Telecommunications CubeSat-Class Spacecraft*, Rijeka, Croatia: INTECH Open Access Publisher, 2010.

[18] J. Heyman. (2009, Oct.). Cubesats—A costing + pricing challenge. *SatMagazine.* [Online]. Available: http://www.satmagazine.com/story.php?number=602922274

[19] The cost of building and launching a satellite. (n.d.). GlobalCom. [Online]. Available:http://www.globalcomsatphone.com/hughesnet/satellite/costs.html. Accessed Jun. 30, 2016.

[20] Polaris project evening star. (n.d.). Iowa State University. [Online]. Available:http://www.polaris.iastate.edu/EveningStar/Unit4/unit4_sub3.htm. Accessed Jul. 12, 2016.

[21] T. Jessa. (2016, Apr. 26). Low earth orbit. [Online]. Available: http://www.universetoday.com/85322/low-earth-orbit/.

[22] J. D. Bossler, J. R. Jensen, R. B. McMaster, and C. Rizos, *Manual of Geospatial Science and Technology,* Boca Raton, FL: CRC Press, 2004.

[23] Geostationary satellite orbit, GEO. (n.d.). Radio Electronics. [Online]. Available: http://www.radio-electronics.com/info/satellite/satellite-orbits/geostationary-earth-orbit.php. Accessed Jun. 30, 2016.

[24] C. Sabol, R. Burns and C. A. McLaughlin, "Satellite formation flying design and evolution," *J. Spacecraft Rockets*, vol. 38, no. 2, pp. 270–278, Mar. 2001.

[25] Spacecraft Gallery. (n.d.). NASA [Online]. Available: http://oco.jpl.nasa.gov/galleries/galleryspacecraft/#gallery. Accessed Jul. 30, 2016.

[26] H. J. Kramer. (n.d.). Flock 1 imaging constellation. [Online]. Available: https://directory.eoportal.org/web/eoportal/satellite-missions/f/flock-1. Accessed Jul 7, 2016.

[27] 12 flock 2E satellites. (n.d.). Spaceflight. [Online]. Available: http://spaceflight101.com/cygnus-oa4/flock-2e/. Accessed Jul. 7, 2016.

[28] Gunter's Space Page Database. Object name Flock-1. [Online]. Available: http://space.skyrocket.de/doc_sdat/flock-1.htm. Accessed Jul.13, 2016.

[29] Gunter's Space Page Database. Object name Lemur-2. [Online]. Available: http://space.skyrocket.de/doc_sdat/lemur-2.html. Accessed: Jul. 15, 2016.

[30] E. Gill, P. Sundaramoorthy, J. Bouwmeester, B. Zandbergen, and R. Reinhard, "Formation flying within a constellation of nano-satellites: The QB50 mission," *Acta Astronaut*., 2013, vol. 82, pp. 110–117.

[31] P. Raja. (2015, Sep. 7). The art of satellite constellation design: what you need to know. [Online]. Available: http://www.astrome.co/web1/blogs/the-art-of-satellite-constellation-design-what-you-need-to-know/

[32] V. A. Chobotov, *Orbital Mechanics.* Reston, VA: Aiaa, 2002.

[33] W. D. Williams, M. Collins, D. M. Boroson, J. Lesh, A. Biswas, R. Orr, L. Schuchman, and O. S. Sands, "RF and optical communications: A comparison of high data rate returns from deep space in the 2020 timeframe," in *Proceedings of 12th Ka and Broadband Communications Conference*, Naples, Italy, 2007.

[34] H. Kaushal and G. Kaddoum. (2015, Jun.). Free space optical communication: Challenges and mitigation techniques. arXiv. [Online]. Available: http://arxiv.org/abs/1506.04836

[35] K. Rainey. (2015, Jul. 30). OPALS: Light beams let data rate soar. [Online]. Available:http://www.nasa.gov/mission_pages/station/research/news/opals_data_rates_soar

[36] A. Arvizu, J. Santos, E. Dom, R. Muraoka, J. Valdes, and F. Mendieta, "ATP subsystem for optical communications on a Cubesat," in *Proceedings of IEEE International Conference on Space Optical Systems and Applications*, 2015, pp. 1–5.

[37] W. Stallings, *Data and Computer Communications.* Upper Saddle River, NJ: Pearson/Prentice Hall, 2007.

[38] T. T. Ha, *Theory and Design of Digital Communication Systems.* Cambridge, England: Cambridge University Press, 2010.

[39] B. Sklar, *Digital Communications*. Upper Saddle River, NJ: Prentice Hall, 2001.

[40] T. T. Ha, *Digital Satellite Communication.* New York City, NY: Tata McGraw-Hill Education, 1990.

[41] R. Goyal, S. Kota, R. Jain, S. Fahmy, B. Vandalore and J. Kallaus (1998). Analysis and simulation of delay and buffer requirements of satellite-ATM networks for TCP/IP traffic. [Online]. Available: http://www.cse.wustl.edu/~jain/papers/ftp/satdelay.pdf

[42] C. Wiedemann and I. P. Vörsmann. (2012, Mar. 21). Space debris–current situation. [Online]. Available: http://www.unoosa.org/pdf/pres/lsc2012/tech-02E.pdf

[43] K. D. Bilimoria and R. A. Krieger, "Slot architecture for separating satellites in sun-synchronous orbits," in *Proceedings AIAA SPACE Conference and Exposition*, 2011, vol. 1, pp. 1110–1122.

[44] H. Klinkrad, J. Alarcon, and N. Sanchez, "Collision avoidance for operational ESA satellites," in *Proceedings of 4th European Conference on Space Debris,* 2005, vol. 587, pp. 509.

[45] L. Qiao, C. Rizos, and A. G. Dempster, "Analysis and comparison of Cubesat lifetime," in *Proceedings of the 12th Australian Space Conference,* 2013, pp. 249–260.

[46] R. Janovsky, M. Kassebom, H. Liibberstedt, O. Romberg, H. Burkhardt, M. Sippel, G. Kriille, and B. Fritsche, "End-of-life de-orbiting strategies for satellites," *Science and Technology Series,* vol. 109, pp. 411–428, 2004.

[47] O. Kara, M. Brunner, R. Birkeland, D. Schor, B. Yağlıoğlu, T. Smith, and A. Hornig, "Communication architecture and international policy recommendations enabling the development of global cubesat space networks," presented at 66th International Astronautical Congress, Jerusalem, Israel, 2015.

[48] J. Puig-Suari, C. Turner, and W. Ahlgren, "Development of the standard CubeSat deployer and a CubeSat class PicoSatellite," in *Proceedings IEEE Aerospace Conference, Big Sky, MT,* 2001, vol. 1, pp. 347–353.

[49] Nanocom communication modules. (n.d.). [Online]. Available: http://www.gomspace.com/index.php?p=products-ax100. Accessed Aug. 15, 2016.

[50] TRX-U UHF transceiver. (n.d.). Spacequest. [Online]. Available: http://www.spacequest.com/radios-and-modems/sqtrx-u. Accessed Aug. 15, 2016.

[51] Z. Tang, Z. Feng, W. Yu, W. Han, B. Zhao, C. Wu, X. Mao and F. Chen, "A quasi-dynamic inter-satellite link reassignment method for LEO satellite networks," presented at International Conference on Wireless Algorithms, Systems, and Applications, Shangdong, China, 2015.

THIS PAGE INTENTIONALLY LEFT BLANK

INITIAL DISTRIBUTION LIST

1. Defense Technical Information Center
   Ft. Belvoir, Virginia

2. Dudley Knox Library
   Naval Postgraduate School
   Monterey, California